

The two-body $B_c \rightarrow D_{(s)}^{(*)}P, D_{(s)}^{(*)}V$ decays in the Perturbative QCD Approach

Zhou Rui, Zhi-Tian Zou, and Cai-Dian Lü*

*Institute of High Energy Physics and Theoretical Physics Center for Science Facilities,
Chinese Academy of Sciences, Beijing 100049, People's Republic of China*

(Dated: October 27, 2018)

Abstract

We make a systematic investigation on the two-body nonleptonic decays $B_c \rightarrow D_{(s)}^{(*)}P, D_{(s)}^{(*)}V$, by employing the perturbative QCD approach based on k_T factorization, where P and V denote any light pseudoscalar meson and vector meson, respectively. We predict the branching ratios and direct CP-asymmetries of these B_c decays and also the transverse polarization fractions of $B_c \rightarrow D_{(s)}^{(*)}V$ decays. It is found that the non-factorizable emission diagrams and annihilation type diagrams have remarkable effects on the physical observables in many channels, especially the color-suppressed and annihilation-dominant decay modes. A possible large direct CP-violation is predicted in some channels; and a large transverse polarization contribution that can reach 50% \sim 70% is predicted in some of the $B_c \rightarrow D_{(s)}^{(*)}V$ decays.

PACS numbers: 13.25.Hw, 12.38.Bx, 14.40.Nd

*Electronic address: lucd@ihep.ac.cn

I. INTRODUCTION

The B_c meson is the only quark-antiquark bound system ($\bar{b}c$) composed of both heavy quarks with different flavors, and are thus flavor asymmetric. It can decay only via weak interaction, since the two flavor asymmetric quarks (b and c) can not annihilate into gluons or photon via strong interaction or electromagnetic interaction. Because each of the two heavy quarks can decay individually, and they can also annihilate through weak interaction, B_c meson has rich decay channels and provides a very good place to study nonleptonic weak decays of heavy mesons, to test the standard model and to search for any new physics signals [1].

Since the current running LHC collider will produce much more B_c mesons than ever before, a lot of theoretical studies of the nonleptonic B_c weak decays have been performed using different approaches. For example, the spectator-model [2], the light-front quark model (LFQM) [3, 4], the relativistic constituent quark model (RCQM) [5], the QCD factorization approach (QCDF) [6], the Perturbative QCD approach (pQCD) [7–10], and so on. Among the numerous decay channels, there is one category with only one charmed meson in the final states. They are rare decays, but with possible large direct CP asymmetry, since there are both penguin and tree diagrams involved. These decays have ever been studied in Ref. [3] using the naive factorization approach. But they consider only the contribution of current-current operators at the tree level, and thus no direct CP asymmetry is predicted. They also have difficulty to predict those pure penguin type or annihilation dominant type decays, such as $B_c \rightarrow D^+\phi$, $D_s^+\bar{K}^0$, $D_s^+\phi$. Ref. [5] discussed some semileptonic and nonleptonic B_c weak decays and CP-violating asymmetries by using RCQM model based on the Bethe-Salpeter formalism. They do not include the contributions of annihilation type diagrams, either. Since the annihilation type contributions are found to be important in the B meson non-leptonic decays [11] and also significant in the B_c decays [12], one needs further study these channels carefully.

In this paper, we calculate all the processes of a B_c meson decays to one $D_{(s)}^{(*)}$ meson and one light pseudoscalar meson (P) or vector meson (V) in pQCD approach. It is well-known that B_c meson is a nonrelativistic heavy quarkonium system. Thus the two quarks in the B_c meson are both at rest and non-relativistic. Since the charm quark in the final state D meson is almost at collinear state, a hard gluon is needed to transfer large momentum

to the spectator charm quark. In the leading order of $m_c/m_{B_c} \sim 0.2$ expansion, the factorization theorem is applicable to the B_c system similar to the situation of B meson [13]. Utilizing the k_T factorization instead of collinear factorization, this approach is free of endpoint singularity. Thus the diagrams including factorizable, nonfactorizable and annihilation type, are all calculable. It has been tested in the study of charmless B meson decays successfully [14], especially for the direct CP asymmetries [15]. For the charmed decays of B meson, it is also demonstrated to be applicable in the leading order of the m_D/m_B expansion [16–21].

Our paper is organized as follows: We review the pQCD factorization approach and then perform the perturbative calculations for these considered decay channels in Sec.II. The numerical results and discussions on the observables are given in Sec.III. The final section is devoted to our conclusions. Some details related functions and the decay amplitudes are given in the Appendix.

II. THEORETICAL FRAMEWORK

For the charmed B_c decays we considered, the weak effective Hamiltonian \mathcal{H}_{eff} for $b \rightarrow q'(q' = d, s)$ transition can be written as [22]

$$\mathcal{H}_{eff} = \frac{G_F}{\sqrt{2}} \left\{ \sum_{q=u,c} \xi_q [(C_1(\mu)O_1^q(\mu) + C_2(\mu)O_2^q(\mu)) + \sum_{i=3}^{10} C_i(\mu)O_i(\mu)] \right\}, \quad (1)$$

with the Cabbibo-Kobayashi-Maskawa (CKM) matrix element $\xi_q = V_{qq'}V_{qb}^*$. $O_i(\mu)$ and $C_i(\mu)$ are the effective four quark operators and their QCD corrected Wilson coefficients, respectively. Their expressions can be found easily for example in Ref. [22].

With these quark level weak operators, the hardest work is left for the matrix element calculation between hadronic states $\langle DM | \mathcal{H}_{eff} | B_c \rangle$. Since both perturbative and non-perturbative QCD are involved, the factorization theorem is required to make the calculation meaningful. The perturbative QCD approach [14] is one of the methods to deal with hadronic B decays based on k_T factorization. At zero recoil of D meson in the semi-leptonic B_c decay, both c and b quark can be described by heavy quark effective theory. However, when the D meson is at maximum recoil, which is the case of two body non-leptonic B_c decay, the final state mesons at the rest frame of B_c meson are collinear, so as to the constituent quarks (c and other light quarks) inside. Since the spectator

c quark in the B_c meson is almost at rest, a hard gluon is then needed to transform it into a collinear object in the final state meson. This makes the perturbative calculations into a 6-quark interaction. In this collinear factorization calculation, endpoint singularity usually appears in some of the diagrams. The QCD factorization approach [23] just parameterize those diagrams with singularity as free parameters; while in the so-called soft-collinear effective theory [24], people separate these incalculable part to an unknown matrix element. In our pQCD approach, we studied these singularity and found that they arise from the endpoint where longitudinal momentum is small. Therefore, the transverse momentum of quarks is no longer negligible. If one pick back the transverse momentum, the result is finite.

Because the intrinsic transverse momentum of quarks is smaller than the b quark mass scale, therefore we have one more scale than the usual collinear factorization. Additional double logarithms appear at the perturbative QCD calculations. These large logarithms will spoil the perturbation expansion, thus a resummation is required. This has been done to give the so called Sudakov form factors [25]. The single logarithm between the W boson mass scale and the factorization scale t in pQCD approach has been absorbed into the Wilson coefficients of four quark operators. The decay amplitude is then factorized into the convolution of the hard subamplitude, the Wilson coefficient and the Sudakov factor with the meson wave functions, all of which are well-defined and gauge invariant. Therefore, the three-scale factorization formula for exclusive nonleptonic B meson decays is then written as

$$C(t) \otimes H(x, t) \otimes \Phi(x) \otimes \exp \left[-s(P, b) - 2 \int_{1/b}^t \frac{d\mu}{\mu} \gamma_q(\alpha_s(\mu)) \right], \quad (2)$$

where $C(t)$ are the corresponding Wilson coefficients. The Sudakov evolution $\exp[-s(P, b)]$ [25] are from the resummation of double logarithms $\ln^2(Pb)$, with P denoting the dominant light-cone component of meson momentum. $\gamma_q = -\alpha_s/\pi$ is the quark anomalous dimension in axial gauge. All non-perturbative components are organized in the form of hadron wave functions $\Phi(x)$, which can be extracted from experimental data or other non-perturbative method. Since non-perturbative dynamics has been factored out, one can evaluate all possible Feynman diagrams for the six-quark amplitude straightforwardly, which include both traditional factorizable and so-called “non-factorizable” contributions. Factorizable and non-factorizable annihilation type diagrams are also calculable without endpoint singularity.

The meson wave function, which describes hadronization of the quark and anti-quark inside the meson, is independent of the specific processes. Using the wave functions determined from other well measured processes, one can make quantitative predictions here. For the light pseudoscalar meson, its wave function can be defined as [26]

$$\Phi(P, x, \xi) = \frac{i}{2N_c} \gamma_5 [P \phi_P^A(x) + m_0 \phi_P^P(x) + \xi m_0 (\not{P} - 1) \phi_P^T(x)], \quad (3)$$

where P is the momentum of the light meson, and x is the momentum fraction of the quark (or anti-quark) inside the meson. When the momentum fraction of the quark (anti-quark) is set to be x , the parameter ξ should be chosen as $+1(-1)$. The distribution amplitudes $\phi_P^A(x)$, $\phi_P^P(x)$ and $\phi_P^T(x)$ are given in Appendix C.

For the light vector mesons, both longitudes (L) and transverse (T) polarizations are involved. Their wave functions are written as [7]

$$\begin{aligned} \Phi_V^L(x) &= \frac{1}{\sqrt{2N_c}} \{M_V \not{\epsilon}_V^{*L} \phi_V(x) + \not{\epsilon}_V^{*L} P \phi_V^t(x) + M_V \phi_V^s(x)\}_{\alpha\beta}, \\ \Phi_V^T(x) &= \frac{1}{\sqrt{2N_c}} \{M_V \not{\epsilon}_V^{*T} \phi_V^\nu(x) + \not{\epsilon}_V^{*T} P \phi_V^T(x) + i M_V \epsilon_{\mu\nu\rho\sigma} \gamma_5 \epsilon_T^{*\nu} n^\rho v^\sigma \phi_V^a(x)\}_{\alpha\beta}, \end{aligned} \quad (4)$$

where $\epsilon_V^{L(T)}$ denotes the longitudinal (transverse) polarization vector. And convention $\epsilon^{0123} = 1$ is adopted for the Levi-Civita tensor. The distributions amplitudes are also presented in Appendix C.

Consisting of two heavy quarks (b,c), the B_c meson is usually treated as a heavy quarkonium system. In the non-relativistic limit, the B_c wave function can be written as [7]

$$\Phi_{B_c}(x) = \frac{if_B}{4N_c} [(P + M_{B_c}) \gamma_5 \delta(x - r_c)], \quad (5)$$

with $r_c = m_c/M_{B_c}$. Here, we only consider one of the dominant Lorentz structure, and neglect another contribution in our calculation [27].

In the heavy quark limit, the two-particle light-cone distribution amplitudes of $D_{(s)}/D_{(s)}^*$ meson are defined as [21]

$$\begin{aligned} \langle D_{(s)}(P_2) | q_\alpha(z) \bar{c}_\beta(0) | 0 \rangle &= \frac{i}{\sqrt{2N_c}} \int_0^1 dx e^{ixP_2 \cdot z} [\gamma_5 (P_2 + m_{D_{(s)}}) \phi_{D_{(s)}}(x, b)]_{\alpha\beta}, \\ \langle D_{(s)}^*(P_2) | q_\alpha(z) \bar{c}_\beta(0) | 0 \rangle &= -\frac{1}{\sqrt{2N_c}} \int_0^1 dx e^{ixP_2 \cdot z} [\not{\epsilon} (P_2 + m_{D_{(s)}^*}) \phi_{D_{(s)}^*}(x, b)]_{\alpha\beta}. \end{aligned} \quad (6)$$

We use the following relations derived from HQET to determine $f_{D_{(s)}^*}$ [28]

$$f_{D_{(s)}^*} = \sqrt{\frac{m_{D_{(s)}}}{m_{D_{(s)}^*}}} f_{D_{(s)}}. \quad (7)$$

For the $D_{(s)}^{(*)}$ meson wave function, we adopt the same model as of the B meson [8]

$$\phi_{D_{(s)}}(x, b) = N_{D_{(s)}} [x(1-x)]^2 \exp \left(-\frac{x^2 m_{D_{(s)}}^2}{2\omega_{D_{(s)}}^2} - \frac{1}{2} \omega_{D_{(s)}}^2 b^2 \right) \quad (8)$$

with shape parameters $\omega_D = 0.6$ for D/D^* meson and $\omega_{D_s} = 0.8$ for D_s/D_s^* meson. Here, a larger ω_{D_s} parameter than ω_D characterize the fact that the s quark in D_s meson carries a larger momentum fraction than the light quark (u, d) in the D meson.

At leading order, there are eight types of diagrams that may contribute to the $B_c \rightarrow D_{(s)}^{(*)} P, D_{(s)}^{(*)} V$ decays as illustrated in Fig.1. The first line are the emission type diagrams, with the first two contributing to the usual form factor; the last two so-called non-factorizable diagrams. The second line are the annihilation type diagrams, with the first two factorizable; the last two non-factorizable.

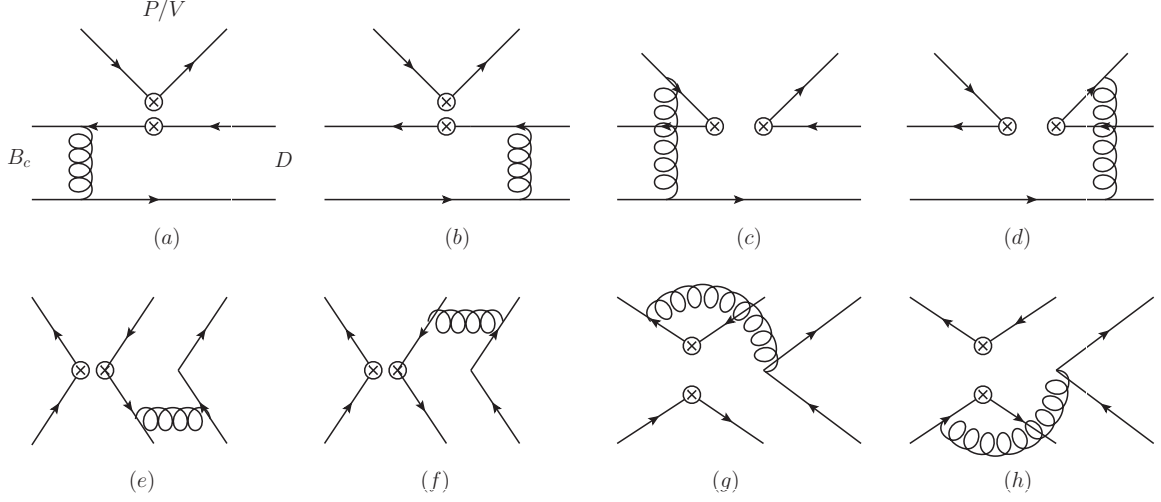


FIG. 1: The leading order Feynman diagrams for the decays $B_c \rightarrow D_{(s)}^{(*)}P, D_{(s)}^{(*)}V$.

A. Amplitudes for $B_c \rightarrow D_{(s)}P$ decays

We mark LL, LR, SP to denote the contributions from $(V-A)(V-A)$, $(V-A)(V+A)$ and $(S-P)(S+P)$ operators, respectively. The amplitudes from factorizable diagrams (a) and (b) in Fig.1 are as following:

$$\begin{aligned}
\mathcal{F}_e^{LL} = & 2\sqrt{\frac{2}{3}}C_F f_B f_P \pi M_B^4 \int_0^1 dx_2 \int_0^\infty db_1 db_2 \phi_D(x_2, b_2) \times \\
& \{[(1-2r_D)x_2 + (r_D-2)r_b]\alpha_s(t_a)h_e(\alpha_e, \beta_a, b_1, b_2)S_t(x_2) \exp[-S_{ab}(t_a)] \\
& -(r_D-2)r_D(x_1-1)\alpha_s(t_b)h_e(\alpha_e, \beta_b, b_2, b_1)S_t(x_1) \exp[-S_{ab}(t_b)]\}, \quad (9)
\end{aligned}$$

where $r_D = m_D/M_B$, $r_b = m_b/M_B$; $C_F = 4/3$ is a color factor; f_P is the decay constant of pseudoscalar meson (P). The factorization scales $t_{a,b}$ are chosen as the maximal virtuality of internal particles in the hard amplitude, in order to suppress the higher order corrections [29]. The function h_e are displayed in the Appendix B. The factor $S_t(x)$ is the jet function from the threshold resummation, whose definitions can be found in [8]. The terms proportional to r_D^2 have been neglected for small values. We can calculate the form

factor from eq.(9) if we take away the Wilson coefficients and f_P . For the $(V - A)(V + A)$ operates, we have $\mathcal{F}_e^{LR} = -\mathcal{F}_e^{LL}$ since only axial-vector current contributes to the pseudoscalar meson production. For the $(S - P)(S + P)$ operates the formula is different:

$$\begin{aligned}\mathcal{F}_e^{SP} = & -4\sqrt{\frac{2}{3}}C_F f_B f_P \pi M_B^4 \int_0^1 dx_2 \int_0^\infty b_1 b_2 db_1 db_2 \phi_D(x_2, b_2) \times \\ & \{[r_D(4r_b - x_2 - 1) - r_b + 2]\alpha_s(t_a)h_e(\alpha_e, \beta_a, b_1, b_2)S_t(x_2) \exp[-S_{ab}(t_a)] \\ & + [r_D(2 - 4x_1) + x_1]\alpha_s(t_b)h_e(\alpha_e, \beta_b, b_2, b_1)S_t(x_1) \exp[-S_{ab}(t_b)]\}.\end{aligned}\quad (10)$$

For the nonfactorizable emission diagram (c) and (d), the decay amplitudes of three types operates are:

$$\begin{aligned}\mathcal{M}_e^{LL} = & \frac{8}{3}C_F f_B \pi M_B^4 \int_0^1 dx_2 dx_3 \int_0^\infty b_2 b_3 db_2 db_3 \phi_D(x_2, b_2) \phi_P^A(x_3) \times \\ & \{[r_D(1 - x_1 - x_2) + x_1 + x_3 - 1]\alpha_s(t_c)h_e(\beta_c, \alpha_e, b_3, b_2) \exp[-S_{cd}(t_c)] - \\ & [r_D(1 - x_1 - x_2) + 2x_1 + x_2 - x_3 - 1]\alpha_s(t_d)h_e(\beta_d, \alpha_e, b_3, b_2) \exp[-S_{cd}(t_d)]\},\end{aligned}\quad (11)$$

$$\begin{aligned}\mathcal{M}_e^{LR} = & \frac{8}{3}C_F f_B \pi M_B^4 r_P (1 + r_D) \int_0^1 dx_2 dx_3 \int_0^\infty b_2 b_3 db_2 db_3 \phi_D(x_2, b_2) \times \\ & \{[(x_1 + x_3 - 1 + r_D(2x_1 + x_2 + x_3 - 2))\phi_P^P(x_3) + \\ & (x_1 + x_3 - 1 + r_D(x_3 - x_2))\phi_P^T(x_3)]\alpha_s(t_c)h_e(\beta_c, \alpha_e, b_3, b_2) \exp[-S_{cd}(t_c)] \\ & - [(x_1 - x_3 + r_D(2x_1 + x_2 - x_3 - 1))\phi_P^P(x_3) + (x_3 - x_1 + \\ & r_D(x_3 + x_2 - 1))\phi_P^T(x_3)]\alpha_s(t_d)h_e(\beta_d, \alpha_e, b_3, b_2) \exp[-S_{cd}(t_d)]\},\end{aligned}\quad (12)$$

$$\begin{aligned}\mathcal{M}_e^{SP} = & \frac{8}{3}C_F f_B \pi M_B^4 \int_0^1 dx_2 dx_3 \int_0^\infty b_2 b_3 db_2 db_3 \phi_D(x_2, b_2) \phi_P^A(x_3) \times \\ & \{[r_D(x_1 + x_2 - 1) - 2x_1 - x_2 - x_3 + 2] \\ & \alpha_s(t_c)h_e(\beta_c, \alpha_e, b_3, b_2) \exp[-S_{cd}(t_c)] - \\ & [x_3 - x_1 - r_D(1 - x_1 - x_2)]\alpha_s(t_d)h_e(\beta_d, \alpha_e, b_3, b_2) \exp[-S_{cd}(t_d)]\},\end{aligned}\quad (13)$$

where $r_P = m_0^P/M_B$, with m_0^P as the chiral mass of the pseudoscalar meson P.

For the factorizable emission diagram (e) and (f), we keep the mass of the c-quark in D meson, while the mass of the light quark is neglected. The amplitudes are given as

follows:

$$\begin{aligned}
\mathcal{F}_a^{LL} = \mathcal{F}_a^{LR} = & -8C_F f_B \pi M_B^4 \int_0^1 dx_2 dx_3 \int_0^\infty b_2 b_3 db_2 db_3 \phi_D(x_2, b_2) \times \\
& \{[\phi_P^A(x_3)(x_3 - 2r_D r_c) + r_P[\phi_P^P(x_3)(2r_D(x_3 + 1) - r_c) + \phi_P^T(x_3) \\
& (r_c + 2r_D(x_3 - 1))]]\alpha_s(t_e)h_e(\alpha_a, \beta_e, b_2, b_3) \exp[-S_{ef}(t_e)]S_t(x_3) - \\
& [x_2 \phi_P^A(x_3) + 2r_P r_D(x_2 + 1)\phi_P^P(x_3)] \\
& \alpha_s(t_f)h_e(\alpha_a, \beta_f, b_3, b_2) \exp[-S_{ef}(t_f)]S_t(x_2)\}, \tag{14}
\end{aligned}$$

$$\begin{aligned}
\mathcal{F}_a^{SP} = & 16C_F f_B \pi M_B^4 \int_0^1 dx_2 dx_3 \int_0^\infty b_2 b_3 db_2 db_3 \phi_D(x_2, b_2) \times \\
& \{[-\phi_P^A(x_3)(2r_D - r_c) + r_P[\phi_P^P(x_3)(4r_c r_D - x_3) + \phi_P^T(x_3)x_3]] \\
& \alpha_s(t_e)h_e(\alpha_a, \beta_e, b_2, b_3) \exp[-S_{ef}(t_e)]S_t(x_3) - [x_2 r_D \phi_P^A(x_3) + \\
& 2r_P \phi_P^P(x_3)]\alpha_s(t_f)h_e(\alpha_a, \beta_f, b_3, b_2) \exp[-S_{ef}(t_f)]S_t(x_2)\}; \tag{15}
\end{aligned}$$

and that of the nonfactorizable annihilation diagram (g) and (h) are

$$\begin{aligned}
\mathcal{M}_a^{LL} = & -\frac{8}{3}C_F f_B \pi M_B^4 \int_0^1 dx_2 dx_3 \int_0^\infty b_1 b_2 db_1 db_2 \phi_D(x_2, b_2) \times \\
& \{[\phi_P^A(x_3)(r_c - x_1 + x_2) + r_P r_D[\phi_P^T(x_3)(x_2 - x_3) + \\
& \phi_P^P(x_3)(4r_c - 2x_1 + x_2 + x_3)]]\alpha_s(t_g)h_e(\beta_g, \alpha_a, b_1, b_2) \exp[-S_{gh}(t_g)] \\
& + [-\phi_P^A(x_3)(r_b + x_1 + x_3 - 1) + r_P r_D[(x_2 - x_3)\phi_P^T(x_3) - \phi_P^P(x_3) \\
& (4r_b + 2x_1 + x_2 + x_3 - 2)]]\alpha_s(t_h)h_e(\beta_h, \alpha_a, b_1, b_2) \exp[-S_{gh}(t_h)]\}, \tag{16}
\end{aligned}$$

$$\begin{aligned}
\mathcal{M}_a^{LR} = & \frac{8}{3}C_F f_B \pi M_B^4 \int_0^1 dx_2 dx_3 \int_0^\infty b_1 b_2 db_1 db_2 \phi_D(x_2, b_2) \times \\
& \{[-\phi_P^A(x_3)r_D(r_c + x_1 - x_2) + r_P[-\phi_P^T(x_3)(-r_c - x_1 + x_3) \\
& + \phi_P^P(x_3)(r_c + x_1 - x_3)]]\alpha_s(t_g)h_e(\beta_g, \alpha_a, b_1, b_2) \exp[-S_{gh}(t_g)] + \\
& [-\phi_P^A(x_3)r_D(-r_b + x_1 + x_2 - 1) + r_P[(-r_b + x_1 + x_3 - 1) \\
& (\phi_P^P(x_3) + \phi_P^T(x_3))]]\alpha_s(t_h)h_e(\beta_h, \alpha_a, b_1, b_2) \exp[-S_{gh}(t_h)]\}, \tag{17}
\end{aligned}$$

$$\begin{aligned}
\mathcal{M}_a^{SP} = & -\frac{8}{3}C_F f_B \pi M_B^4 \int_0^1 dx_2 dx_3 \int_0^\infty b_1 b_2 db_1 db_2 \phi_D(x_2, b_2) \times \\
& \{[-\phi_P^A(x_3)(x_1 - x_3 - r_c) + r_P r_D[-\phi_P^T(x_3)(x_2 - x_3) \\
& + \phi_P^P(x_3)(4r_c - 2x_1 + x_2 + x_3)]]\alpha_s(t_g)h_e(\beta_g, \alpha_a, b_1, b_2) \exp[-S_{gh}(t_g)] + \\
& [-\phi_P^A(x_3)(r_b + x_1 + x_2 - 1) + r_P r_D[(-4r_b - 2x_1 - x_2 - x_3 + 2)\phi_P^P(x_3) \\
& - (x_2 - x_3)\phi_P^T(x_3)]]\alpha_s(t_h)h_e(\beta_h, \alpha_a, b_1, b_2) \exp[-S_{gh}(t_h)]\}, \tag{18}
\end{aligned}$$

With the functions obtained in the above, the total decay amplitudes of 10 decay channels for the $B_c \rightarrow D_{(s)}P$ can be given by

$$\begin{aligned}
\mathcal{A}(B_c \rightarrow D^0 \pi^+) &= \xi_u[a_1 \mathcal{F}_e^{LL} + C_1 \mathcal{M}_e^{LL}] + \xi_c[a_1 \mathcal{F}_a^{LL} + C_1 \mathcal{M}_a^{LL}] \\
&\quad - \xi_t[(C_3 + C_9)(\mathcal{M}_e^{LL} + \mathcal{M}_a^{LL}) + (C_5 + C_7)(\mathcal{M}_e^{LR} + \mathcal{M}_a^{LR}) \\
&\quad + (C_4 + \frac{1}{3}C_3 + C_{10} + \frac{1}{3}C_9)(\mathcal{F}_a^{LL} + \mathcal{F}_e^{LL}) \\
&\quad + (C_6 + \frac{1}{3}C_5 + C_8 + \frac{1}{3}C_7)(\mathcal{F}_a^{SP} + \mathcal{F}_e^{SP})], \tag{19}
\end{aligned}$$

$$\begin{aligned}
\sqrt{2}\mathcal{A}(B_c \rightarrow D^+ \pi^0) &= \xi_u[a_2 \mathcal{F}_e^{LL} + C_2 \mathcal{M}_e^{LL}] - \xi_c[a_1 \mathcal{F}_a^{LL} \\
&\quad + C_1 \mathcal{M}_a^{LL}] - \xi_t[\frac{3}{2}C_{10} - C_3 + \frac{1}{2}C_9)\mathcal{M}_e^{LL} - (C_3 + C_9)\mathcal{M}_a^{LL} \\
&\quad + (-C_5 + \frac{1}{2}C_7)\mathcal{M}_e^{LR} + (-C_4 - \frac{1}{3}C_3 - C_{10} - \frac{1}{3}C_9)\mathcal{F}_a^{LL} + \\
&\quad (C_{10} + \frac{5}{3}C_9 - \frac{1}{3}C_3 - C_4 - \frac{3}{2}C_7 - \frac{1}{2}C_8)\mathcal{F}_e^{LL} \\
&\quad + (-C_6 - \frac{1}{3}C_5 + \frac{1}{2}C_8 + \frac{1}{6}C_7)\mathcal{F}_e^{SP} - (C_5 + C_7)\mathcal{M}_a^{LR} \\
&\quad + (-C_6 - \frac{1}{3}C_5 - C_8 - \frac{1}{3}C_7)\mathcal{F}_a^{SP}], \tag{20}
\end{aligned}$$

$$\begin{aligned}
\sqrt{2}\mathcal{A}(B_c \rightarrow D^+ \eta_q) &= \xi_u[a_2 \mathcal{F}_e^{LL} + C_2 \mathcal{M}_e^{LL}] + \xi_c[a_1 \mathcal{F}_a^{LL} + C_1 \mathcal{M}_a^{LL}] \\
&\quad - \xi_t[(2C_4 + C_3 + \frac{1}{2}C_{10} - \frac{1}{2}C_9)\mathcal{M}_e^{LL} + (C_3 + C_9)\mathcal{M}_a^{LL} \\
&\quad + (C_5 - \frac{1}{2}C_7)\mathcal{M}_e^{LR} + (C_5 + C_7)\mathcal{M}_a^{LR} + (C_4 + \frac{1}{3}C_3 + C_{10} + \\
&\quad \frac{1}{3}C_9)\mathcal{F}_a^{LL} + (\frac{7}{3}C_3 + \frac{5}{3}C_4 + \frac{1}{3}(C_9 - C_{10}))\mathcal{F}_e^{LL} + (2C_5 + \frac{2}{3}C_6 \\
&\quad + \frac{1}{2}C_7 + \frac{1}{6}C_8)\mathcal{F}_e^{LR} + (C_6 + \frac{1}{3}C_5 - \frac{1}{2}C_8 - \frac{1}{6}C_7)\mathcal{F}_e^{SP} \\
&\quad + (C_6 + \frac{1}{3}C_5 + C_8 + \frac{1}{3}C_7)\mathcal{F}_a^{SP}], \tag{21}
\end{aligned}$$

$$\begin{aligned}
\mathcal{A}(B_c \rightarrow D^+ \eta_s) &= -\xi_t[(C_4 - \frac{1}{2}C_{10})\mathcal{M}_e^{LL} + (C_6 - \frac{1}{2}C_8)\mathcal{M}_e^{SP} + (C_3 + \frac{1}{3}C_4 \\
&\quad - \frac{1}{2}C_9 - \frac{1}{6}C_{10})\mathcal{F}_e^{LL} + (C_5 + \frac{1}{3}C_6 - \frac{1}{2}C_7 - \frac{1}{6}C_8)\mathcal{F}_e^{LR}], \tag{22}
\end{aligned}$$

$$\begin{aligned}
\sqrt{2}\mathcal{A}(B_c \rightarrow D_s^+ \eta_q) &= \xi'_u[a_2 \mathcal{F}_e^{LL} + C_2 \mathcal{M}_e^{LL}] - \xi'_t[(2C_4 + \frac{1}{2}C_{10})\mathcal{M}_e^{LL} + \\
&\quad (2C_6 + \frac{1}{2}C_8)\mathcal{M}_e^{SP} + (2C_3 + \frac{2}{3}C_4 + \frac{1}{2}C_9 + \frac{1}{6}C_{10})\mathcal{F}_e^{LL} \\
&\quad + (2C_5 + \frac{2}{3}C_6 + \frac{1}{2}C_7 + \frac{1}{6}C_8)\mathcal{F}_e^{LR}], \tag{23}
\end{aligned}$$

$$\begin{aligned}
\mathcal{A}(B_c \rightarrow D_s^+ \eta_s) = & \xi'_c[a_1 \mathcal{F}_a^{LL} + C_1 \mathcal{M}_a^{LL}] - \xi'_t[(C_3 + C_4 - \frac{1}{2}(C_{10} + C_9))\mathcal{M}_e^{LL} \\
& + (C_3 + C_9)\mathcal{M}_a^{LL} + (C_5 - \frac{1}{2}C_7)\mathcal{M}_e^{LR} + (C_5 + C_7)\mathcal{M}_a^{LR} \\
& + (C_4 + \frac{1}{3}C_3 + C_{10} + \frac{1}{3}C_9)\mathcal{F}_a^{LL} + (C_6 - \frac{1}{2}C_8)\mathcal{M}_e^{SP} + \\
& \frac{2}{3}(2(C_3 + C_4) - (C_9 + C_{10}))\mathcal{F}_e^{LL} + (C_5 + \frac{1}{3}C_6 - \frac{1}{2}C_7 - \frac{1}{6}C_8)\mathcal{F}_e^{LR} \\
& + (C_6 + \frac{1}{3}C_5 - \frac{1}{2}C_8 - \frac{1}{6}C_7)\mathcal{F}_e^{SP} + (C_6 + \frac{1}{3}C_5 + C_8 + \frac{1}{3}C_7)\mathcal{F}_a^{SP}],
\end{aligned} \tag{24}$$

$$\begin{aligned}
\mathcal{A}(B_c \rightarrow D_s^+ \bar{K}^0) = & \xi_c[a_1 \mathcal{F}_a^{LL} + C_1 \mathcal{M}_a^{LL}] - \xi_t[(C_3 - \frac{1}{2}C_9)\mathcal{M}_e^{LL} \\
& + (C_3 + C_9)\mathcal{M}_a^{LL} + (C_5 - \frac{1}{2}C_7)\mathcal{M}_e^{LR} + (C_5 + C_7)\mathcal{M}_a^{LR} \\
& + (C_4 + \frac{1}{3}C_3 + C_{10} + \frac{1}{3}C_9)\mathcal{F}_a^{LL} + \\
& (C_4 + \frac{1}{3}C_3 - \frac{1}{2}C_{10} - \frac{1}{6}C_9)\mathcal{F}_e^{LL} + (C_6 + \frac{1}{3}C_5 - \frac{1}{2}C_8 \\
& - \frac{1}{6}C_7)\mathcal{F}_e^{SP} + (C_6 + \frac{1}{3}C_5 + C_8 + \frac{1}{3}C_7)\mathcal{F}_a^{SP}],
\end{aligned} \tag{25}$$

$$\begin{aligned}
\mathcal{A}(B_c \rightarrow D_s^+ \pi^0) = & \xi'_u[a_2 \mathcal{F}_e^{LL} + C_2 \mathcal{M}_e^{LL}] - \xi'_t[(\frac{1}{2}(3C_9 + C_{10})\mathcal{F}_e^{LL} \\
& + \frac{1}{2}(3C_7 + C_8))\mathcal{F}_e^{LR} + \frac{3}{2}C_{10}\mathcal{M}_e^{LL} + \frac{3}{2}C_8\mathcal{M}_e^{SP}],
\end{aligned} \tag{26}$$

with the CKM matrix element $\xi_i = V_{id}V_{ib}^*$ and $\xi'_i = V_{is}V_{ib}^*$ ($i = u, c, t$). The combinations Wilson coefficients $a_1 = C_2 + C_1/3$ and $a_2 = C_1 + C_2/3$. The total decay amplitude of $\mathcal{A}(B_c \rightarrow D^0 K^+)$ and $\mathcal{A}(B_c \rightarrow D^+ K^0)$ can be obtained from (19) and (25), respectively, with the following replacement:

$$\begin{aligned}
\mathcal{A}(B_c \rightarrow D^0 K^+) &= \mathcal{A}(B_c \rightarrow D^0 \pi^+) |_{\pi \rightarrow K, \xi_i \rightarrow \xi'_i}, \\
\mathcal{A}(B_c \rightarrow D^+ K^0) &= \mathcal{A}(B_c \rightarrow D_s^+ \bar{K}^0) |_{D_s \rightarrow D, \xi_i \rightarrow \xi'_i}.
\end{aligned} \tag{27}$$

It should be noticed that, in (21), (22), (23) and (24), the decay amplitudes are for the mixing basis of (η_q, η_s) . For the physical state (η, η') , the decay amplitudes are

$$\begin{aligned}
\mathcal{A}(B_c \rightarrow D^+ \eta) &= \mathcal{A}(B_c \rightarrow D^+ \eta_q) \cos \phi - \mathcal{A}(B_c \rightarrow D^+ \eta_s) \sin \phi, \\
\mathcal{A}(B_c \rightarrow D^+ \eta') &= \mathcal{A}(B_c \rightarrow D^+ \eta_q) \sin \phi + \mathcal{A}(B_c \rightarrow D^+ \eta_s) \cos \phi, \\
\mathcal{A}(B_c \rightarrow D_s^+ \eta) &= \mathcal{A}(B_c \rightarrow D_s^+ \eta_q) \cos \phi - \mathcal{A}(B_c \rightarrow D_s^+ \eta_s) \sin \phi, \\
\mathcal{A}(B_c \rightarrow D_s^+ \eta') &= \mathcal{A}(B_c \rightarrow D_s^+ \eta_q) \sin \phi + \mathcal{A}(B_c \rightarrow D_s^+ \eta_s) \cos \phi,
\end{aligned} \tag{28}$$

where $\phi = 39.3^\circ$ is the mixing angle between the two states.

$$\begin{pmatrix} \eta \\ \eta' \end{pmatrix} = \begin{pmatrix} \cos \phi & -\sin \phi \\ \sin \phi & \cos \phi \end{pmatrix} \begin{pmatrix} \eta_q \\ \eta_s \end{pmatrix}. \quad (29)$$

B. Amplitudes for $B_c \rightarrow D_{(s)}V$ decays

In $B_c \rightarrow D_{(s)}V$ decays, the vector meson is longitudinally polarized. In the leading power contribution, the formula of each Feynman diagram for $B_c \rightarrow D_{(s)}V$ is similar to that of the $B_c \rightarrow D_{(s)}P$ modes, but with the replacements

$$f_P \rightarrow f_V, \quad r_P \rightarrow r_V, \quad \phi_P^A \rightarrow \phi_V, \quad \phi_P^P \rightarrow -\phi_V^s, \quad \phi_P^T \rightarrow \phi_V^t. \quad (30)$$

The total decay amplitude for $B_c \rightarrow D_{(s)}V$ can be obtained through the substitutions in (19)- (27):

$$\pi \rightarrow \rho, \quad K \rightarrow K^*, \quad \eta_q \rightarrow \omega, \quad \eta_s \rightarrow \phi. \quad (31)$$

C. Amplitudes for $B_c \rightarrow D_{(s)}^*V$ decays

The decay amplitude of $B_c \rightarrow D_{(s)}^*V$ can be decomposed into

$$\mathcal{A}(\epsilon_{D^*}, \epsilon_V) = \mathcal{A}^L + \mathcal{A}^N \epsilon_{D^*T} \cdot \epsilon_{VT} + i\mathcal{A}^T \epsilon_{\alpha\beta\rho\sigma} n^\alpha v^\beta \epsilon_{D^*T}^\rho \epsilon_{VT}^\sigma \quad (32)$$

where $\epsilon_{D^*T}(\epsilon_{VT})$ is the transverse polarization vector for $D^*(V)$ meson. \mathcal{A}^L corresponds to the contributions of longitudinal polarization; \mathcal{A}^N and \mathcal{A}^T corresponds to the contributions of normal and transverse polarization, respectively. The factorization formulae for the longitudinal, normal and transverse polarizations are all listed in Appendix A. There are also 10 channels for $B_c \rightarrow D_{(s)}^*V$ decay modes. We can obtain the total decay amplitudes from those in $B_c \rightarrow D_{(s)}V$ with replacing $D_{(s)}$ by $D_{(s)}^*$.

D. Amplitudes for $B_c \rightarrow D_{(s)}^*P$ decays

For $B_c \rightarrow D_{(s)}^*P$, only the longitudinal polarization of $D_{(s)}^*$ will contribute. We can obtain their amplitudes from the longitudinal polarization amplitudes for the $B_c \rightarrow D_{(s)}^*V$ decays with the following replacement in the distribution amplitudes:

$$f_V \rightarrow f_P, \quad r_V \rightarrow r_P, \quad \phi_V \rightarrow \phi_P^A, \quad \phi_V^s \rightarrow \phi_P^P, \quad \phi_V^t \rightarrow \phi_P^T. \quad (33)$$

TABLE I: The decay constants and the hadronic meson wave function parameters taken from the light-cone sum rules [33].

| The decay constants (MeV) | | | | | | | | | | | | |
|------------------------------|-----------------|-----------------|----------|-------|----------|------------|------------|--------------|----------|------------|-----------|-------------|
| f_{B_c} | f_D | f_{D_s} | f_π | f_K | f_ρ | f_ρ^T | f_ω | f_ω^T | f_ϕ | f_ϕ^T | f_{K^*} | $f_{K^*}^T$ |
| 489 | 206.7 ± 8.9 | 257.5 ± 6.1 | 131 | 160 | 209 | 165 | 195 | 145 | 231 | 200 | 217 | 185 |
| Values of Gegenbauer moments | | | | | | | | | | | | |
| | π | K | η_q | | η_s | | | | | | | |
| a_1^P | — | 0.17 | — | | — | | | | | | | |
| a_2^P | 0.25 | 0.115 | 0.115 | | 0.115 | | | | | | | |
| a_4^P | -0.015 | -0.015 | -0.015 | | -0.015 | | | | | | | |
| | ρ | ω | ϕ | | K^* | | | | | | | |
| a_1^\parallel | — | — | — | | 0.03 | | | | | | | |
| a_2^\parallel | 0.15 | 0.15 | 0.18 | | 0.11 | | | | | | | |
| a_1^\perp | — | — | — | | 0.04 | | | | | | | |
| a_2^\perp | 0.14 | 0.14 | 0.14 | | 0.10 | | | | | | | |

In fact, the $B_c \rightarrow D_{(s)}^* P$ decays amplitude are the same as the $B_c \rightarrow D_{(s)} P$ ones only at leading power under the hierarchy $M_{B_c} \gg m_{D^{(*)}} \gg \Lambda_{QCD}$. An explicit derivation shows that the difference between the two kinds of channels occurs at $\mathcal{O}(r_{D^{(*)}})$ and at the twist-3 level in eq.(9)-eq.(18).

III. NUMERICAL RESULTS AND DISCUSSIONS

The numerical results of our calculations depend on a set of input parameters. We list the decay constants of various mesons and parameters of hadronic wave functions in Table I. For $\eta - \eta'$ system, the decay constants f_q and f_s in the quark-flavor basis have been extracted from various related experiments [30, 31]

$$f_q = (1.07 \pm 0.02)f_\pi, \quad f_s = (1.34 \pm 0.06)f_\pi. \quad (34)$$

For the CKM matrix elements, the quark masses etc., we adopt the results from [32]

$$\begin{aligned}
|V_{ub}| &= (3.89 \pm 0.44) \times 10^{-3}, & |V_{ud}| &= 0.97425, & |V_{cb}| &= 0.0406, & |V_{cd}| &= 0.23 \\
|V_{us}| &= 0.2252, & |V_{cs}| &= 1.023, & \gamma &= (73_{-25}^{+22})^\circ, \\
m_c &= 1.27\text{GeV}, & m_b &= 4.2\text{GeV}, & m_0^\pi &= 1.4\text{GeV}, \\
m_0^K &= 1.6\text{GeV}, & m_0^{\eta_q} &= 1.07\text{GeV}, & m_0^{\eta_s} &= 1.92\text{GeV}, & \Lambda_{QCD}^5 &= 0.112\text{GeV}.
\end{aligned} \quad (35)$$

For the considered $B_c \rightarrow D_{(s)}P$, $B_c \rightarrow D_{(s)}^*P$ and $B_c \rightarrow D_{(s)}V$ decays, the branching ratios \mathcal{BR} and the direct CP asymmetry A_{CP}^{dir} for a given mode can be written as

$$\mathcal{BR} = \frac{G_F \tau_{B_c}}{32\pi M_B} (1 - r_D^2) |\mathcal{A}|^2, \quad A_{CP}^{dir} = \frac{|\bar{\mathcal{A}}|^2 - |\mathcal{A}|^2}{|\bar{\mathcal{A}}|^2 + |\mathcal{A}|^2} \quad (36)$$

where the decay amplitudes \mathcal{A} have been given explicitly in Sec. II for each channel. $\bar{\mathcal{A}}$ is the corresponding charge conjugate decay amplitude, which can be obtained by conjugating the CKM matrix elements in \mathcal{A} .

Our numerical results of CP averaged branching ratios and direct CP asymmetries for $B_c \rightarrow D_{(s)}P$ and $B_c \rightarrow D_{(s)}V$ decays are listed in Tables II and III, respectively. The dominant topologies contributing to these decays are also indicated through the symbols T (color-allowed tree), C (color-suppressed tree), P (penguin) and A (annihilation). The first theoretical error in all our tables is referred to the $D_{(s)}$ meson wave function: (1) The shape parameter $\omega_D = 0.60 \pm 0.05$ for D/D^* meson and $\omega_{D_s} = 0.80 \pm 0.05$ for D_s/D_s^* meson; (2) The decay constant $f_D = (206.7 \pm 8.9)\text{MeV}$ for D meson and $f_{D_s} = (257.5 \pm 6.1)\text{MeV}$ for D_s meson. The second error is from the combined uncertainty in the CKM matrix elements V_{ub} and the angle of unitarity triangle γ , which are given in eq.(35). The third error arises from the hard scale t varying from $0.75t$ to $1.25t$, which characterizing the size of next-to-leading order QCD contributions. Most of the branching ratios are sensitive to the hadronic parameters and the CKM matrix elements. The CP asymmetry parameter is only sensitive to the next-to-leading order contributions, since the uncertainty of hadronic parameters are mostly canceled by the ratios.

We also cite theoretical results for the relevant decays evaluated in LFQM model [3] and RCQM model [5] to make a comparison in Tables II and III. Our pQCD results are generally close to RCQM results but differ substantially from the ones obtained by LFQM. This is due to the fact that LFQM used a smaller form factors $F^{B_c \rightarrow D}(q^2 = 0) = 0.086$ at maximum recoil, which is rather smaller than other model predictions [4] and also another covariant LFQM results [34]. In fact, these model calculations all give consistent form factors at the zero recoil region, considering only soft contributions by the overlap between the initial and final state meson wave functions, which is good at the zero recoil region. At the maximum-recoil region, which is the case for non-leptonic B decays, the soft contribution is suppressed, since a hard gluon is needed, as discussed in the previous section. Furthermore LFQM only consider the contribution of current-current operators at the tree level, therefore they cannot give predictions for those modes without tree diagram

TABLE II: CP averaged branching ratios and direct CP asymmetries for $B_c \rightarrow D_{(s)}P$ decays, together with results from RCQM and LFQM.

| channels | Class | $\mathcal{BR}(10^{-7})$ | | | $A_{CP}^{dir}(\%)$ | |
|----------------------------------|-------|--|-------------------|--------|--|------|
| | | This work | RCQM ^a | LFQM | This work | RCQM |
| $B_c \rightarrow D^0\pi^+$ | T | $26.7^{+3.1+6.0+0.8}_{-3.5-5.6-0.6}$ | 22.9 | 4.3 | $-41.2^{+4.5+11.1+0.8}_{-4.6-7.8-1.2}$ | 6.5 |
| $B_c \rightarrow D^+\pi^0$ | C,A | $0.82^{+0.24+0.55+0.06}_{-0.16-0.41-0.01}$ | 2.1 | 0.067 | $2.3^{+6.3+1.4+15.0}_{-3.0-0.8-18.8}$ | -1.9 |
| $B_c \rightarrow D^0K^+$ | A,P | $47.8^{+17.2+2.2+5.4}_{-9.1-1.7-3.6}$ | 44.5 | 0.35 | $-34.8^{+4.9+7.4+1.8}_{-2.6-3.7-1.3}$ | -4.6 |
| $B_c \rightarrow D^+K^0$ | A,P | $46.9^{+15.6+0.3+7.4}_{-12.3-0.3-4.6}$ | 49.3 | — | $2.3^{+0.4+0.9+0.0}_{-0.2-0.5-0.0}$ | -0.8 |
| $B_c \rightarrow D^+\eta$ | C,A | $0.92^{+0.15+0.21+0.03}_{-0.15-0.25-0.00}$ | — | 0.087 | $40.8^{+0.0+18.4+15.6}_{-2.9-14.0-13.5}$ | — |
| $B_c \rightarrow D^+\eta'$ | C,A | $0.91^{+0.12+0.16+0.06}_{-0.10-0.20-0.03}$ | — | 0.048 | $-14.0^{+0.6+4.6+15.9}_{-1.5-5.2-11.9}$ | — |
| $B_c \rightarrow D_s^+\pi^0$ | C,P | $0.41^{+0.04+0.01+0.02}_{-0.04-0.02-0.02}$ | — | 0.0067 | $46.7^{+1.4+6.3+2.5}_{-1.4-11.8-2.8}$ | — |
| $B_c \rightarrow D_s^+\bar{K}^0$ | A,P | $2.1^{+0.9+0.3+0.3}_{-0.6-0.3-0.2}$ | 1.9 | — | $54.3^{+6.9+5.3+0.0}_{-7.2-8.0-0.3}$ | 13.3 |
| $B_c \rightarrow D_s^+\eta$ | A,P | $17.3^{+1.7+0.5+3.3}_{-1.8-0.6-1.2}$ | — | 0.009 | $2.8^{+0.0+0.4+1.1}_{-0.1-0.7-1.2}$ | — |
| $B_c \rightarrow D_s^+\eta'$ | A,P | $51.0^{+4.9+0.4+6.7}_{-5.4-0.3-3.5}$ | — | 0.0048 | $1.1^{+0.1+0.2+0.7}_{-0.0-0.2-0.6}$ | — |

^awe use the results of decay widths in [5], but we take $\tau_{B_c} = 0.453\text{ps}$ to estimate the branching ratio

TABLE III: CP averaged branching ratios and direct CP asymmetries for $B_c \rightarrow D_{(s)}V$ decays, together with results from RCQM and LFQM.

| channels | Class | $\mathcal{BR}(10^{-7})$ | | | $A_{CP}^{dir}(\%)$ | |
|-------------------------------------|-------|---|------|--------|--|------|
| | | This work | RCQM | LFQM | This work | RCQM |
| $B_c \rightarrow D^0\rho^+$ | T | $66.2^{+7.6+16.0+1.6}_{-7.6-14.1-1.3}$ | 60.0 | 13 | $-24.5^{+2.6+5.3+0.3}_{-0.4-3.2-0.8}$ | 3.8 |
| $B_c \rightarrow D^+\rho^0$ | C,A | $1.4^{+0.1+0.5+0.1}_{-0.2-0.5-0.2}$ | 3.9 | 0.2 | $79.8^{+0.3+11.2+3.4}_{-5.8-19.6-10.7}$ | -3.0 |
| $B_c \rightarrow D^0K^{*+}$ | A,P | $25.9^{+2.7+0.9+1.5}_{-3.0-0.8-0.8}$ | 34.7 | 0.68 | $-66.2^{+1.8+15.1+0.7}_{-0.6-6.5-0.0}$ | -6.2 |
| $B_c \rightarrow D^+K^{*0}$ | A,P | $19.1^{+3.3+0.1+0.7}_{-2.5-0.0-0.7}$ | 28.8 | — | $3.5^{+0.0+0.5+0.5}_{-0.1-0.8-0.3}$ | -0.8 |
| $B_c \rightarrow D^+\omega$ | C,A | $1.9^{+0.3+0.5+0.0}_{-0.3-0.6-0.0}$ | — | 0.15 | $-3.6^{+3.9+1.3+13.4}_{-1.2-1.6-10.7}$ | — |
| $B_c \rightarrow D^+\phi$ | P | $0.008^{+0.001+0.0+0.001}_{-0.001-0.0-0.001}$ | — | — | — | — |
| $B_c \rightarrow D_s^+\rho^0$ | C,P | $0.95^{+0.10+0.02+0.04}_{-0.09-0.01-0.04}$ | — | — | $50.2^{+1.0+5.9+2.5}_{-1.1-11.9-3.2}$ | — |
| $B_c \rightarrow D_s^+\bar{K}^{*0}$ | A,P | $1.4^{+0.2+0.0+0.1}_{-0.2-0.1-0.1}$ | 1.0 | — | $61.0^{+0.0+6.5+4.5}_{-0.3-14.2-3.6}$ | 13.3 |
| $B_c \rightarrow D_s^+\omega$ | C,P | $0.31^{+0.03+0.07+0.07}_{-0.03-0.07-0.05}$ | — | 0.016 | $44.9^{+0.8+17.1+10.3}_{-1.6-14.9-13.6}$ | — |
| $B_c \rightarrow D_s^+\phi$ | A,P | $27.0^{+4.8+0.1+2.0}_{-1.2-0.0-0.4}$ | 15.7 | 0.0048 | $3.3^{+0.0+0.4+0.3}_{-0.3-0.8-0.4}$ | -0.8 |

contributions like $B_c \rightarrow D^+K^0$ and $B_c \rightarrow D_s^+\bar{K}^0$. For the color suppressed decays (C), our predictions differ from the ones of RCQM, since in these modes, the contributions from the non-factorizable emission diagram and annihilation diagram dominated the branching ratio, which are not calculable in RCQM.

Our numerical results of the CP averaged branching ratios and direct CP asymmetries for $B_c \rightarrow D_{(s)}^*P$ decays are listed in Table IV, together with the RCQM model predictions.

Again, our results are similar with RCQM model for the tree dominant mode (T). But for the annihilation dominant and penguin dominant modes (A,P), the branching ratios obtained in the RCQM are one order of magnitude smaller than ours. The reason is that these decay amplitudes are governed by the QCD penguin parameters a_4 and a_6 in the combination $a_4 + Ra_6$ [35] in the factorization hypothesis. The coefficient R arises from the penguin operator O_6 , where $R > 0$ for $B \rightarrow PP$, $R = 0$ for PV and VV final states, and $R < 0$ for $B \rightarrow VP$, the second meson in the final states is the one emitted from vacuum. Therefore, the branching ratios of various type decays have the following pattern in the factorization approach

$$\mathcal{BR}(B_c \rightarrow DP) > \mathcal{BR}(B_c \rightarrow DV) \sim \mathcal{BR}(B_c \rightarrow D^*V) > \mathcal{BR}(B_c \rightarrow D^*P) \quad (37)$$

as a consequence of the interference between the a_4 and a_6 penguin terms. In the contrary, we have additional non-factorization contributions and large annihilation type contributions in the pQCD approach, which spoils the relation in eq.(37).

As expected, the annihilation type diagrams give large contributions in the B_c meson decays, because the annihilation type diagram contributions are enhanced by the CKM factor $V_{cb}^*V_{cq}$ [7, 36]. For the $b \rightarrow d$ process, $|\frac{V_{cb}^*V_{cd}}{V_{ub}^*V_{ud}}| = 2.5$; For the $b \rightarrow s$ process, $|\frac{V_{cb}^*V_{cs}}{V_{ub}^*V_{us}}| = 47$. The annihilation diagram contributions are the dominant contribution in some $b \rightarrow s$ processes. Therefore, we have the ratio relation $\frac{\mathcal{BR}(B_c \rightarrow D^{(*)0}K^{(*)+})}{\mathcal{BR}(B_c \rightarrow D^{(*)+}K^{(*)0})} \approx 1$ for these two annihilation dominant $b \rightarrow s$ transition processes.

For the color suppressed decays (C), our predictions differ from the ones of RCQM, since in these modes, the contributions from the non-factorizable emission diagram and annihilation diagram dominated the branching ratio, which are not calculable in RCQM. For example in decays $B_c \rightarrow D^{(*)+}(\pi^0, \eta, \eta', \rho^0, \omega)$, the non-factorizable contribution, which is proportional to the large Wilson coefficient C_2 , is the dominant contribution. In fact, the annihilation diagrams can also give relatively large contributions for the enhancement by CKM factor. We also find that the twist-3 distribution amplitudes play an important role, especially in the factorizable annihilation diagrams. As stated in section IID, the $B_c \rightarrow DP(V)$ decay amplitudes are different from $B_c \rightarrow D^*P(V)$ ones only at twist-3 level. The numerical results show that the contributions from factorizable annihilation diagrams have an opposite sign between the two type channels. For example, this results in a constructive interference between non-factorizable emission diagrams and factorizable annihilation diagrams for $B_c \rightarrow D^{*+}\pi^0$, but a destructive interference

TABLE IV: CP averaged branching ratios and direct CP asymmetries for $B_c \rightarrow D_{(s)}^* P$ decays, together with results from RCQM.

| | | $\mathcal{BR}(10^{-7})$ | | $A_{CP}^{dir}(\%)$ | |
|-------------------------------------|-------|--|------|---|------|
| channels | Class | This work | RCQM | This work | RCQM |
| $B_c \rightarrow D^{*0}\pi^+$ | T | $18.8^{+2.0+4.1+0.4}_{-2.0-3.5-0.5}$ | 19.6 | $64.0^{+12.0+6.1+0.7}_{-7.6-13.0-0.5}$ | 1.5 |
| $B_c \rightarrow D^{*+}\pi^0$ | C,A | $1.3^{+0.4+0.2+0.0}_{-0.3-0.3-0.0}$ | 0.66 | $9.6^{+3.3+3.4+10.8}_{-2.7-3.3-8.8}$ | -2.1 |
| $B_c \rightarrow D^{*0}K^+$ | A,P | $73.5^{+31.0+0.8+0.7}_{-23.4-1.1-0.4}$ | 4.9 | $25.0^{+4.4+3.2+0.1}_{-4.1-6.1-0.3}$ | -8.2 |
| $B_c \rightarrow D^{*+}K^0$ | A,P | $77.8^{+25.4+0.2+7.2}_{-24.0-0.2-5.2}$ | 2.8 | $-0.3^{+0.0+0.0+0.0}_{-0.0-0.0-0.0}$ | -8.2 |
| $B_c \rightarrow D^{*+}\eta$ | C,A | $0.34^{+0.14+0.19+0.04}_{-0.09-0.15-0.00}$ | — | $-2.0^{+0.0+0.7+22.8}_{-2.4-1.5-30.0}$ | — |
| $B_c \rightarrow D^{*+}\eta'$ | C,A | $0.15^{+0.08+0.08+0.03}_{-0.05-0.06-0.01}$ | — | $-41.8^{+17.5+13.0+24.3}_{-24.5-13.0-19.2}$ | — |
| $B_c \rightarrow D_s^{*+}\pi^0$ | C,P | $0.27^{+0.02+0.03+0.01}_{-0.04-0.02-0.02}$ | — | $29.9^{+2.4+5.3+1.8}_{-1.9-8.2-1.5}$ | — |
| $B_c \rightarrow D_s^{*+}\bar{K}^0$ | A,P | $1.6^{+0.2+0.1+0.2}_{-0.3-0.1-0.1}$ | 0.21 | $-3.3^{+0.4+0.6+0.9}_{-1.0-0.4-0.4}$ | 13.3 |
| $B_c \rightarrow D_s^{*+}\eta$ | A,P | $16.7^{+5.3+0.3+0.1}_{-4.0-0.2-0.3}$ | — | $-0.7^{+0.2+0.2+0.6}_{-0.2-0.0-0.3}$ | — |
| $B_c \rightarrow D_s^{*+}\eta'$ | A,P | $14.4^{+6.6+0.1+0.5}_{-4.6-0.1-0.6}$ | — | $0.02^{+0.01+0.00+0.55}_{-0.02-0.01-0.52}$ | — |

TABLE V: CP averaged branching ratios, direct CP asymmetries and the transverse polarization fractions for $B_c \rightarrow D_{(s)}^* V$ decays, together with results from RCQM.

| | | $\mathcal{BR}(10^{-7})$ | | $A_{CP}^{dir}(\%)$ | | $\mathcal{R}_T(\%)$ |
|--|-------|--|------|---------------------------------------|------|---------------------------------------|
| channels | Class | This work | RCQM | This work | RCQM | This work |
| $B_c \rightarrow D^{*0}\rho^+$ | T | $55.3^{+8.6+11.9+1.5}_{-5.0-11.1-1.4}$ | 59.7 | $-24.1^{+3.0+4.2+0.4}_{-3.4-2.7-0.4}$ | 3.8 | $16.4^{+2.5+2.0+0.3}_{-1.7-1.4-0.1}$ |
| $B_c \rightarrow D^{*+}\rho^0$ | C,A | $3.8^{+1.0+0.5+0.1}_{-0.8-0.6-0.1}$ | 13.0 | $30.2^{+0.0+2.6+5.4}_{-1.5-5.8-7.6}$ | -3.0 | $54.3^{+1.8+4.0+0.5}_{-0.9-2.4-0.4}$ |
| $B_c \rightarrow D^{*0}K^{*+}$ | A,P | $161^{+59+5+11}_{-40-4-9}$ | 37.7 | $-14.9^{+1.1+3.1+0.3}_{-0.8-1.7-0.1}$ | -6.2 | $52.6^{+1.5+2.3+1.3}_{-1.1-1.8-0.7}$ |
| $B_c \rightarrow D^{*+}K^{*0}$ | A,P | $172^{+57+1+11}_{-42-1-9}$ | 30.6 | $0.4^{+0.0+0.0+0.0}_{-0.0-0.1-0.0}$ | -0.8 | $57.4^{+0.6+0.1+0.9}_{-0.7-0.1-0.4}$ |
| $B_c \rightarrow D^{*+}\omega$ | C,A | $2.4^{+0.4+0.9+0.2}_{-0.6-0.7-0.1}$ | — | $-7.8^{+1.0+2.6+5.8}_{-0.0-3.4-5.0}$ | — | $56.0^{+1.2+9.6+0.7}_{-0.5-6.5-0.7}$ |
| $B_c \rightarrow D^{*+}\phi$ | P | $0.004^{+0.001+0+0}_{-0-0-0.001}$ | — | — | — | $11.4^{+22.3+0.0+5.3}_{-5.4-0.0-6.9}$ |
| $B_c \rightarrow D_s^{*+}\rho^0$ | C,P | $0.72^{+0.08+0.03+0.02}_{-0.08-0.03-0.03}$ | — | $-29.3^{+1.3+7.6+1.4}_{-1.1-4.5-0.9}$ | -3.0 | $11.2^{+0.5+2.1+0.2}_{-0.3-1.4-0.1}$ |
| $B_c \rightarrow D_s^{*+}\bar{K}^{*0}$ | A,P | $4.3^{+1.3+0.4+0.3}_{-1.0-0.3-0.2}$ | 2.9 | $6.2^{+0.1+1.3+0.0}_{-0.3-1.8-0.1}$ | 13.3 | $68.8^{+2.1+3.9+0.8}_{-2.3-4.4-0.4}$ |
| $B_c \rightarrow D_s^{*+}\omega$ | C,P | $0.26^{+0.03+0.04+0.07}_{-0.01-0.05-0.04}$ | — | $-21.3^{+5.3+6.8+7.9}_{-4.6-6.8-4.7}$ | — | $49.5^{+8.8+2.1+4.4}_{-10.9-1.2-2.8}$ |
| $B_c \rightarrow D_s^{*+}\phi$ | A,P | $137.3^{+39.3+0.5+10.5}_{-27.8-0.5-7.5}$ | 38.8 | $0.3^{+0.1+0.1+0.0}_{-0.1-0.1-0.0}$ | -0.8 | $67.5^{+2.1+0.1+1.4}_{-3.1-0.2-1.5}$ |

for $B_c \rightarrow D^+\pi^0$. This makes $\mathcal{BR}(B_c \rightarrow D^{*+}\pi^0)$ larger than $\mathcal{BR}(B_c \rightarrow D^+\pi^0)$. Similarly, we have $\mathcal{BR}(B_c \rightarrow D^{*+}\rho^0) > \mathcal{BR}(B_c \rightarrow D^+\rho^0)$. However, for $B_c \rightarrow D^{(*)+}\eta(\eta')$, while the $d\bar{d}$ part contributes to the annihilation diagrams, the constructive or destructive interference situation are just the reverse, and $\mathcal{BR}(B_c \rightarrow D^{*+}\eta(\eta'))$ are smaller than $\mathcal{BR}(B_c \rightarrow D^+\eta(\eta'))$.

For another kind of $b \rightarrow s$ processes, the decays $B_c \rightarrow D_s^{(*)+}(\pi^0, \rho^0, \omega)$ have a small branching ratio at $\mathcal{O}(10^{-8})$ due to the absent annihilation diagram contributions, and the

emission diagram contributions suppressed by CKM matrix elements $|V_{ub}^* V_{us}|$. Since the contribution of penguin operator is comparable to the one of tree operator, the interference between the two contributions is large. As a result, a big CP asymmetry is predicted in these decays. The branching ratio is even smaller $\sim 10^{-10}$ and no CP violation for $B_c \rightarrow D^{(*)+} \phi$ decays, since there are only penguin diagrams contributions. All these and other rare decays are also important, since they are quite sensitive to new physics contributions.

For the $B_c \rightarrow D_{(s)}^* V$ decays the branching ratios and the transverse polarization fractions \mathcal{R}_T are given as

$$\mathcal{BR} = \frac{G_F^2 \tau_{B_c}}{32\pi M_B} (1 - r_D^2) \sum_{i=0,+,-} |\mathcal{A}_i|^2, \quad \mathcal{R}_T = \frac{|\mathcal{A}_+|^2 + |\mathcal{A}_-|^2}{|\mathcal{A}_0|^2 + |\mathcal{A}_+|^2 + |\mathcal{A}_-|^2}, \quad (38)$$

where the helicity amplitudes \mathcal{A}_i have the following relationships with $\mathcal{A}^{L,N,T}$

$$\mathcal{A}_0 = \mathcal{A}^L, \quad \mathcal{A}_\pm = \mathcal{A}^N \pm \mathcal{A}^T. \quad (39)$$

Our numerical results of the CP averaged branching ratios, direct CP asymmetries and the transverse polarization fractions for $B_c \rightarrow D_{(s)}^* V$ decays are shown in Table V. The transverse polarization contributions are usually suppressed by the factor r_V or r_{D^*} comparing with the longitudinal polarization contributions, thus we do have relatively small transverse polarization fractions for the tree-dominant decay ($\mathcal{R}_T(B_c \rightarrow D^{*0} \rho^+) = 16.4\%$) and the pure penguin type decay ($\mathcal{R}_T(B_c \rightarrow D^{*+} \phi) = 11.5\%$). For the pure emission type decay $B_c \rightarrow D_s^{*+} \omega$, the transverse polarization fraction is large because the non-factorizable emission diagram induced by operator O_6 can enhance the transverse polarization sizably. The fact that the non-factorizable contribution can give large transverse polarization contribution is also observed in the $B^0 \rightarrow \rho^0 \rho^0, \omega \omega$ decays [37]. For other decays, the annihilation type contributions dominate the branching ratios due to the large Wilson coefficients. Therefore, the transverse polarizations take a larger ratio in the branching ratios, which can reach $50\% \sim 70\%$. This is similar to the case of $B \rightarrow \phi K^*$ and various $B \rightarrow \rho K^*$ decays [38, 39].

From Table V, one can also see that our branching ratios for $B_c \rightarrow D^{*+} K^{*0}, D^{*0} K^{*+}, D_s^{*+} \bar{K}^{*0}, D_s^{*+} \phi$ decays, are about 2 to 5 times larger than those in RCQM model, due to the sizable contributions of transverse polarization amplitudes. Another point should be addressed that the annihilation contributions with a strong phase

have remarkable effects on the direct CP asymmetries in these decays. As a result, our predictions are somewhat larger than those from RCQM.

IV. CONCLUSION

In this paper, we investigate the two body non-leptonic decays of B_c meson with the final states involving one $D_{(s)}^{(*)}$ meson in the pQCD approach based on k_T factorization. It is found that the non-factorizable emission and annihilation type diagrams are possible to give a large contribution, especially for those color suppressed modes and annihilation diagram dominant modes. All the branching ratios and CP asymmetry parameters are calculated and the ratios of the transverse polarization contributions in the $B_c \rightarrow D_{(s)}^* V$ decays are estimated. Because of the different weak phase and strong phase from tree diagrams, penguin diagrams and annihilation diagrams, we predict a possible large direct CP-violation in some channels. We also find that the transverse polarization contributions in some channels, which mainly come from the non-factorizable emission diagrams or annihilation type diagrams, are large.

Generally, our predictions for the branching ratios in the tree-dominant B_c decays are in good agreements with that of RCQM model. But we have much larger branching ratios in the color-suppressed, annihilation diagram dominant B_c decays, due to the included non-factorizable diagrams and annihilation type diagrams contributions.

Acknowledgments

We thank Hsiang-nan Li and Fusheng Yu for helpful discussions. This work is partially supported by National Natural Science Foundation of China under the Grant No. 10735080, and 11075168; Natural Science Foundation of Zhejiang Province of China, Grant No. Y606252 and Scientific Research Fund of Zhejiang Provincial Education Department of China, Grant No. 20051357.

Appendix A: factorization formulas for $B_c \rightarrow D^*V$

We mark L, N and T to denote the contributions from longitudinal polarization, normal polarization and transverse polarization, respectively.

$$\begin{aligned}\mathcal{F}_e^{LL,L} = & 2\sqrt{\frac{2}{3}}\pi C_f f_B f_V M_B^4 \int_0^1 dx_2 \int_0^\infty b_1 b_2 db_1 db_2 \phi_{D(s)}^*(x_2, b_2) \times \\ & \{[x_2 - 2r_b + r_D(r_b - 2x_2)]\alpha_s(t_a)h_e(\alpha_e, \beta_a, b_1, b_2)S_t(x_2) \exp[-S_{ab}(t_a)] \\ & + [r_D^2(x_1 - 1)]\alpha_s(t_b)h_e(\alpha_e, \beta_b, b_2, b_1)S_t(x_1) \exp[-S_{ab}(t_b)]\},\end{aligned}\quad (\text{A1})$$

$$\begin{aligned}\mathcal{F}_e^{LL,N} = & 2\sqrt{\frac{2}{3}}\pi C_f f_B f_V M_B^4 r_V \int_0^1 dx_2 \int_0^\infty b_1 b_2 db_1 db_2 \phi_{D(s)}^*(x_2, b_2) \times \\ & \{[r_b - 2 + r_D(x_2 + 1 - 4r_b)]\alpha_s(t_a)h_e(\alpha_e, \beta_a, b_1, b_2)S_t(x_2) \exp[-S_{ab}(t_a)] \\ & + r_D[2x_1 - 1]\alpha_s(t_b)h_e(\alpha_e, \beta_b, b_2, b_1)S_t(x_1) \exp[-S_{ab}(t_b)]\},\end{aligned}\quad (\text{A2})$$

$$\begin{aligned}\mathcal{F}_e^{LL,T} = & 2\sqrt{\frac{2}{3}}\pi C_f f_B f_V M_B^4 r_V \int_0^1 dx_2 \int_0^\infty b_1 b_2 db_1 db_2 \phi_{D(s)}^*(x_2, b_2) \times \\ & \{[r_b - 2 + r_D(1 - x_2)]\alpha_s(t_a)h_e(\alpha_e, \beta_a, b_1, b_2)S_t(x_2) \exp[-S_{ab}(t_a)] \\ & - r_D\alpha_s(t_b)h_e(\alpha_e, \beta_b, b_2, b_1)S_t(x_1) \exp[-S_{ab}(t_b)]\},\end{aligned}\quad (\text{A3})$$

$$\mathcal{F}_e^{LR,L} = \mathcal{F}_e^{LL,L}, \quad \mathcal{F}_e^{LR,N} = \mathcal{F}_e^{LL,N}, \quad \mathcal{F}_e^{LR,T} = \mathcal{F}_e^{LL,T}.\quad (\text{A4})$$

The factorizable emission topology contribution $\mathcal{F}_e^{SP,i}(i = L, N, T)$ vanishes due to the conservation of charge parity.

$$\begin{aligned}\mathcal{M}_e^{LL,L} = & -\frac{8}{3}\pi C_f f_B M_B^4 \int_0^1 dx_2 dx_3 \int_0^\infty b_2 b_3 db_2 db_3 \phi_{D(s)}^*(x_2, b_2) \phi_V(x_3) \{[1 - x_1 \\ & - x_3 - r_D(x_1 + x_2 - 1)]\alpha_s(t_c)h_e(\beta_c, \alpha_e, b_3, b_2) \exp[-S_{cd}(t_c)] + [-1 + 2x_1 \\ & + x_2 - x_3 - r_D(x_1 + x_2 - 1)]\alpha_s(t_d)h_e(\beta_d, \alpha_e, b_3, b_2) \exp[-S_{cd}(t_d)]\},\end{aligned}\quad (\text{A5})$$

$$\begin{aligned}\mathcal{M}_e^{LL,N} = & \frac{8}{3}\pi C_f f_B M_B^4 r_V \int_0^1 dx_2 dx_3 \int_0^\infty b_2 b_3 db_2 db_3 \phi_{D(s)}^*(x_2, b_2) \{[(x_1 + x_3 - 1) \\ & \phi_V^\nu(x_3) + 2r_D(x_3 - x_2)\phi_V^a(x_3)]\alpha_s(t_c)h_e(\beta_c, \alpha_e, b_3, b_2) \exp[-S_{cd}(t_c)] \\ & - [(-2r_D(1 - 2x_1 - x_2 + x_3) - x_1 + x_3)\phi_V^\nu(x_3) + 2(r_D(1 - x_2 - x_3) \\ & - 2x_1 + 2x_3)\phi_V^a(x_3)]\alpha_s(t_d)h_e(\beta_d, \alpha_e, b_3, b_2) \exp[-S_{cd}(t_d)]\},\end{aligned}\quad (\text{A6})$$

$$\begin{aligned}
\mathcal{M}_e^{LL,T} = & \frac{8}{3}\pi C_f f_B M_B^4 r_V \int_0^1 dx_2 dx_3 \int_0^\infty b_2 b_3 db_2 db_3 \phi_{D(s)}^*(x_2, b_2) \times \\
& \{[(x_1 + x_3 - 1)\phi_V^\nu(x_3) - 2r_D(2x_1 + x_2 + x_3 - 2)\phi_V^a(x_3)] \\
& \alpha_s(t_c) h_e(\beta_c, \alpha_e, b_3, b_2) \exp[-S_{cd}(t_c)] \\
& - [(x_3 - x_1)\phi_V^\nu(x_3) + 2(r_D(2x_1 + x_2 - x_3 - 1) - 2x_1 + 2x_3)\phi_V^a(x_3)] \\
& \alpha_s(t_d) h_e(\beta_d, \alpha_e, b_3, b_2) \exp[-S_{cd}(t_d)]\}, \tag{A7}
\end{aligned}$$

$$\begin{aligned}
\mathcal{M}_e^{LR,L} = & -\frac{8}{3}\pi C_f f_B M_B^4 \int_0^1 dx_2 dx_3 \int_0^\infty b_2 b_3 db_2 db_3 \phi_{D(s)}^*(x_2, b_2) \phi_V(x_3) \times \\
& \{[(x_1 + x_3 - 1 + r_D(x_2 - x_3))\phi_V^s(x_3) + (x_1 + x_3 - 1 - \\
& r_D(2x_1 + x_2 + x_3 - 2))\phi_V^t(x_3)]\alpha_s(t_c) h_e(\beta_c, \alpha_e, b_3, b_2) \exp[-S_{cd}(t_c)] \\
& - [(x_1 - x_3 - r_D(1 - x_2 - x_3))\phi_V^s(x_3) - (x_1 - x_3 + r_D(1 - 2x_1 \\
& - x_2 + x_3))\phi_V^t(x_3)]\alpha_s(t_d) h_e(\beta_d, \alpha_e, b_3, b_2) \exp[-S_{cd}(t_d)]\}, \tag{A8}
\end{aligned}$$

$$\begin{aligned}
\mathcal{M}_e^{LR,T} = \mathcal{M}_e^{LR,N} = & -\frac{8}{3}\pi C_f f_B M_B^4 r_D \int_0^1 dx_2 dx_3 \int_0^\infty b_2 b_3 db_2 db_3 \phi_{D(s)}^*(x_2, b_2) \\
& \phi_V^T(x_3) (x_1 + x_2 - 1) \{ \alpha_s(t_c) h_e(\beta_c, \alpha_e, b_3, b_2) \exp[-S_{cd}(t_c)] \\
& + \alpha_s(t_d) h_e(\beta_d, \alpha_e, b_3, b_2) \exp[-S_{cd}(t_d)] \}, \tag{A9}
\end{aligned}$$

$$\begin{aligned}
\mathcal{M}_e^{SP,L} = & -\frac{8}{3}\pi C_f f_B M_B^4 \int_0^1 dx_2 dx_3 \int_0^\infty b_2 b_3 db_2 db_3 \phi_{D(s)}^*(x_2, b_2) \phi_V(x_3) \{ [2 - 2x_1 \\
& - x_2 - x_3 + r_D(x_1 + x_2 - 1)] \alpha_s(t_c) h_e(\beta_c, \alpha_e, b_3, b_2) \exp[-S_{cd}(t_c)] - \\
& [x_3 - x_1 - r_D(x_1 + x_2 - 1)] \alpha_s(t_d) h_e(\beta_d, \alpha_e, b_3, b_2) \exp[-S_{cd}(t_d)] \}, \tag{A10}
\end{aligned}$$

$$\begin{aligned}
\mathcal{M}_e^{SP,N} = & -\frac{8}{3}\pi C_f f_B M_B^4 r_V \int_0^1 dx_2 dx_3 \int_0^\infty b_2 b_3 db_2 db_3 \phi_{D(s)}^*(x_2, b_2) \times \\
& \{ [(x_1 + x_3 - 1 - 2r_D(2x_1 + x_2 + x_3 - 2))\phi_V^\nu(x_3) - (x_1 + x_3 - 1)\phi_V^a(x_3)] \\
& \alpha_s(t_c) h_e(\beta_c, \alpha_e, b_3, b_2) \exp[-S_{cd}(t_c)] \\
& + (x_1 - x_3)(\phi_V^\nu(x_3) - \phi_V^a(x_3)) \alpha_s(t_d) h_e(\beta_d, \alpha_e, b_3, b_2) \exp[-S_{cd}(t_d)] \}, \tag{A11}
\end{aligned}$$

$$\begin{aligned}
\mathcal{M}_e^{SP,T} = & \frac{8}{3}\pi C_f f_B M_B^4 r_V \int_0^1 dx_2 dx_3 \int_0^\infty b_2 b_3 db_2 db_3 \phi_{D(s)}^*(x_2, b_2) \times \\
& \{ [(x_1 + x_3 - 1 - 2r_D(2x_1 + x_2 + x_3 - 2))\phi_V^a(x_3) - (x_1 + x_3 - 1)\phi_V^\nu(x_3)] \\
& \alpha_s(t_c) h_e(\beta_c, \alpha_e, b_3, b_2) \exp[-S_{cd}(t_c)] \\
& + (x_1 - x_3)(\phi_V^a(x_3) - \phi_V^\nu(x_3)) \alpha_s(t_d) h_e(\beta_d, \alpha_e, b_3, b_2) \exp[-S_{cd}(t_d)] \}, \tag{A12}
\end{aligned}$$

$$\begin{aligned}
\mathcal{F}_a^{LL,L} = & 8C_F f_B \pi M_B^4 \int_0^1 dx_2 dx_3 \int_0^\infty b_2 b_3 db_2 db_3 \phi_{D(s)}^*(x_2, b_2) \{ [-x_3 \phi_V(x_3) \\
& + r_c r_V (\phi_V^t(x_3) - \phi_V^s(x_3))] \alpha_s(t_e) h_e(\alpha_a, \beta_e, b_2, b_3) \exp[-S_{ef}(t_e)] S_t(x_3) + \\
& [x_2 \phi_V(x_3) + 2r_V r_D (x_2 - 1) \phi_V^s(x_3)] \\
& \alpha_s(t_f) h_e(\alpha_a, \beta_f, b_3, b_2) \exp[-S_{ef}(t_f)] S_t(x_2) \}, \tag{A13}
\end{aligned}$$

$$\begin{aligned}
\mathcal{F}_a^{LL,N} = & -8C_F f_B \pi M_B^4 r_D \int_0^1 dx_2 dx_3 \int_0^\infty b_2 b_3 db_2 db_3 \phi_{D(s)}^*(x_2, b_2) \{ [r_V (x_3 - 1) \phi_V^a(x_3) \\
& - r_c \phi_V^T(x_3) + r_V (x_3 + 1) \phi_V^\nu] \alpha_s(t_e) h_e(\alpha_a, \beta_e, b_2, b_3) \exp[-S_{ef}(t_e)] S_t(x_3) \\
& - r_V [(x_2 + 1) \phi_V^\nu(x_3) - (x_2 - 1) \phi_V^a(x_3)] \\
& \alpha_s(t_f) h_e(\alpha_a, \beta_f, b_3, b_2) \exp[-S_{ef}(t_f)] S_t(x_2) \}, \tag{A14}
\end{aligned}$$

$$\begin{aligned}
\mathcal{F}_a^{LL,T} = & 8C_F f_B \pi M_B^4 r_D \int_0^1 dx_2 dx_3 \int_0^\infty b_2 b_3 db_2 db_3 \phi_{D(s)}^*(x_2, b_2) \times \\
& \{ [r_V (x_3 + 1) \phi_V^a(x_3) - r_c \phi_V^T(x_3) + r_V (x_3 - 1) \phi_V^\nu(x_3)] \\
& \alpha_s(t_e) h_e(\alpha_a, \beta_e, b_2, b_3) \exp[-S_{ef}(t_e)] S_t(x_3) \\
& + r_V [(-x_2 - 1) \phi_V^a(x_3) + (x_2 - 1) \phi_V^\nu(x_3)] \\
& \alpha_s(t_f) h_e(\alpha_a, \beta_f, b_3, b_2) \exp[-S_{ef}(t_f)] S_t(x_2) \}, \tag{A15}
\end{aligned}$$

$$\mathcal{F}_a^{LR,L} = \mathcal{F}_a^{LL,L}, \quad \mathcal{F}_a^{LR,N} = \mathcal{F}_a^{LL,N}, \quad \mathcal{F}_a^{LR,T} = \mathcal{F}_a^{LL,T}, \tag{A16}$$

$$\begin{aligned}
\mathcal{F}_a^{SP,L} = & 16C_F f_B \pi M_B^4 \int_0^1 dx_2 dx_3 \int_0^\infty b_2 b_3 db_2 db_3 \phi_{D(s)}^*(x_2, b_2) \{ [r_c \phi_V(x_3) \\
& + r_V x_3 (\phi_V^s(x_3) - \phi_V^t(x_3))] \alpha_s(t_e) h_e(\alpha_a, \beta_e, b_2, b_3) \exp[-S_{ef}(t_e)] - \\
& [r_D x_2 \phi_V(x_3) - 2r_V \phi_V^s(x_3)] \alpha_s(t_f) h_e(\alpha_a, \beta_f, b_3, b_2) \exp[-S_{ef}(t_f)] \}, \tag{A17}
\end{aligned}$$

$$\begin{aligned}
\mathcal{F}_a^{SP,N} = & -16C_F f_B \pi M_B^4 \int_0^1 dx_2 dx_3 \int_0^\infty b_2 b_3 db_2 db_3 \phi_{D(s)}^*(x_2, b_2) \times \\
& \{ r_D [\phi_V^T(x_3) - 2r_c r_V \phi_V^\nu(x_3)] \alpha_s(t_e) h_e(\alpha_a, \beta_e, b_2, b_3) \exp[-S_{ef}(t_e)] \\
& + r_V (\phi_V^\nu(x_3) + \phi_V^a(x_3)) \alpha_s(t_f) h_e(\alpha_a, \beta_f, b_3, b_2) \exp[-S_{ef}(t_f)] \}, \tag{A18}
\end{aligned}$$

$$\begin{aligned}
\mathcal{F}_a^{SP,T} = & -16C_F f_B \pi M_B^4 \int_0^1 dx_2 dx_3 \int_0^\infty b_2 b_3 db_2 db_3 \phi_{D(s)}^*(x_2, b_2) \times \\
& \{ r_D [\phi_V^T(x_3) - 2r_c r_V \phi_V^a(x_3)] \alpha_s(t_e) h_e(\alpha_a, \beta_e, b_2, b_3) \exp[-S_{ef}(t_e)] \\
& + r_V (\phi_V^\nu(x_3) + \phi_V^a(x_3)) \alpha_s(t_f) h_e(\alpha_a, \beta_f, b_3, b_2) \exp[-S_{ef}(t_f)] \}, \tag{A19}
\end{aligned}$$

$$\begin{aligned}
\mathcal{M}_a^{LL,L} = & \frac{8}{3}C_F f_B \pi M_B^4 \int_0^1 dx_2 dx_3 \int_0^\infty b_1 b_2 db_1 db_2 \phi_{D_{(s)}^*}(x_2, b_2) \{ [(x_1 - x_2 - r_c) \\
& \phi_V(x_3) - r_D r_V [(x_2 - x_3) \phi_V^s(x_3) - (2x_1 - x_2 - x_3) \phi_V^t(x_3)] \\
& \alpha_s(t_g) h_e(\beta_g, \alpha_a, b_1, b_2) \exp[-S_{gh}(t_g)] - [(1 - r_b - x_1 - x_3) \phi_V(x_3) \\
& - r_D r_V [(x_3 - x_2) \phi_V^s(x_3) + (2x_1 + x_2 + x_3 - 2) \phi_V^t(x_3)] \\
& \alpha_s(t_h) h_e(\beta_h, \alpha_a, b_1, b_2) \exp[-S_{gh}(t_h)] \}, \tag{A20}
\end{aligned}$$

$$\begin{aligned}
\mathcal{M}_a^{LL,N} = & -\frac{16}{3}C_F f_B \pi M_B^4 r_D r_V \int_0^1 dx_2 dx_3 \int_0^\infty b_1 b_2 db_1 db_2 \phi_{D_{(s)}^*}(x_2, b_2) \phi_V^\nu(x_3) \times \\
& \{ r_c \alpha_s(t_g) h_e(\beta_g, \alpha_a, b_1, b_2) \exp[-S_{gh}(t_g)] \\
& - r_b \alpha_s(t_h) h_e(\beta_h, \alpha_a, b_1, b_2) \exp[-S_{gh}(t_h)] \}, \tag{A21}
\end{aligned}$$

$$\begin{aligned}
\mathcal{M}_a^{LL,T} = & -\frac{16}{3}C_F f_B \pi M_B^4 r_D r_V \int_0^1 dx_2 dx_3 \int_0^\infty b_1 b_2 db_1 db_2 \phi_{D_{(s)}^*}(x_2, b_2) \phi_V^a(x_3) \times \\
& \{ r_c \alpha_s(t_g) h_e(\beta_g, \alpha_a, b_1, b_2) \exp[-S_{gh}(t_g)] \\
& - r_b \alpha_s(t_h) h_e(\beta_h, \alpha_a, b_1, b_2) \exp[-S_{gh}(t_h)] \}, \tag{A22}
\end{aligned}$$

$$\begin{aligned}
\mathcal{M}_a^{LR,L} = & \frac{8}{3}C_F f_B \pi M_B^4 \int_0^1 dx_2 dx_3 \int_0^\infty b_1 b_2 db_1 db_2 \phi_{D_{(s)}^*}(x_2, b_2) \{ [r_D(x_1 - x_2 + r_c) \\
& \phi_V(x_3) + r_V(-x_1 + x_3 - r_c)(\phi_V^s(x_3) + \phi_V^t(x_3))] \\
& \alpha_s(t_g) h_e(\beta_g, \alpha_a, b_1, b_2) \exp[-S_{gh}(t_g)] - [-r_D(x_1 + x_2 - r_b - 1) \phi_V(x_3) \\
& + r_V(x_1 + x_3 - r_b - 1)(\phi_V^s(x_3) + \phi_V^t(x_3))] \\
& \alpha_s(t_h) h_e(\beta_h, \alpha_a, b_1, b_2) \exp[-S_{gh}(t_h)] \}, \tag{A23}
\end{aligned}$$

$$\begin{aligned}
\mathcal{M}_a^{LR,T} = \mathcal{M}_a^{LR,N} = & \frac{8}{3}C_F f_B \pi M_B^4 \int_0^1 dx_2 dx_3 \int_0^\infty b_1 b_2 db_1 db_2 \phi_{D_{(s)}^*}(x_2, b_2) \times \\
& \{ [r_V(x_1 - x_3 + r_c)(\phi_V^\nu(x_3) + \phi_V^a(x_3)) - r_D(x_1 - x_2 + r_c) \phi_V^T(x_3)] \\
& \alpha_s(t_g) h_e(\beta_g, \alpha_a, b_1, b_2) \exp[-S_{gh}(t_g)] + \\
& [r_V(x_1 + x_3 - r_b - 1)(\phi_V^\nu(x_3) + \phi_V^a(x_3)) + r_D(1 + r_b - x_1 - x_2) \phi_V^T(x_3)] \\
& \alpha_s(t_h) h_e(\beta_h, \alpha_a, b_1, b_2) \exp[-S_{gh}(t_h)] \}, \tag{A24}
\end{aligned}$$

$$\begin{aligned}
\mathcal{M}_a^{SP,L} = & \frac{8}{3} C_F f_B \pi M_B^4 \int_0^1 dx_2 dx_3 \int_0^\infty b_1 b_2 db_1 db_2 \phi_{D(s)}^*(x_2, b_2) \{ [(x_1 - x_3 - r_c) \\
& \phi_V(x_3) - r_D r_V [(x_3 - x_2) \phi_V^s(x_3) - (2x_1 - x_2 - x_3) \phi_V^t(x_3)]] \\
& \alpha_s(t_g) h_e(\beta_g, \alpha_a, b_1, b_2) \exp[-S_{gh}(t_g)] - [(1 - r_b - x_1 - x_2) \phi_V(x_3) \\
& - r_D r_V [(x_2 - x_3) \phi_V^s(x_3) + (2x_1 + x_2 + x_3 - 2) \phi_V^t(x_3)]] \\
& \alpha_s(t_h) h_e(\beta_h, \alpha_a, b_1, b_2) \exp[-S_{gh}(t_h)] \}, \tag{A25}
\end{aligned}$$

$$\mathcal{M}_a^{SP,N} = \mathcal{M}_a^{LL,N}, \quad \mathcal{M}_a^{SP,T} = -\mathcal{M}_a^{LL,T}. \tag{A26}$$

Appendix B: scales and related functions in hard kernel

We show here the functions h_e , coming from the Fourier transform of hard kernel.

$$\begin{aligned}
h_e(\alpha, \beta, b_1, b_2) &= h_1(\alpha, b_1) \times h_2(\beta, b_1, b_2), \\
h_1(\alpha, b_1) &= \begin{cases} K_0(\sqrt{\alpha} b_1), & \alpha > 0 \\ K_0(i\sqrt{-\alpha} b_1), & \alpha < 0 \end{cases} \\
h_2(\beta, b_1, b_2) &= \begin{cases} \theta(b_1 - b_2) I_0(\sqrt{\beta} b_2) K_0(\sqrt{\beta} b_1) + (b_1 \leftrightarrow b_2), & \beta > 0 \\ \theta(b_1 - b_2) J_0(\sqrt{-\beta} b_2) K_0(i\sqrt{-\beta} b_1) + (b_1 \leftrightarrow b_2), & \beta < 0 \end{cases} \tag{B1}
\end{aligned}$$

where J_0 is the Bessel function and K_0, I_0 are modified Bessel function with $K_0(ix) = \frac{\pi}{2}(-N_0(x) + iJ_0(x))$. The hard scale t is chosen as the maximum of the virtuality of the internal momentum transition in the hard amplitudes, including $1/b_i (i = 1, 2, 3)$:

$$\begin{aligned}
t_a &= \max(\sqrt{|\alpha_e|}, \sqrt{|\beta_a|}, 1/b_1, 1/b_2), & t_b &= \max(\sqrt{|\alpha_e|}, \sqrt{|\beta_b|}, 1/b_1, 1/b_2), \\
t_c &= \max(\sqrt{|\alpha_e|}, \sqrt{|\beta_c|}, 1/b_2, 1/b_3), & t_d &= \max(\sqrt{|\alpha_e|}, \sqrt{|\beta_d|}, 1/b_2, 1/b_3), \\
t_e &= \max(\sqrt{|\alpha_a|}, \sqrt{|\beta_e|}, 1/b_2, 1/b_3), & t_f &= \max(\sqrt{|\alpha_a|}, \sqrt{|\beta_f|}, 1/b_2, 1/b_3), \\
t_g &= \max(\sqrt{|\alpha_a|}, \sqrt{|\beta_g|}, 1/b_1, 1/b_2), & t_h &= \max(\sqrt{|\alpha_a|}, \sqrt{|\beta_h|}, 1/b_1, 1/b_2), \tag{B2}
\end{aligned}$$

where

$$\begin{aligned}
\alpha_e &= (1 - x_1 - x_2)(x_1 - r_D^2)M_B^2, & \alpha_a &= -x_2 x_3 (1 - r_D^2)M_B^2, \\
\beta_a &= [r_b^2 - x_2(1 - r_D^2)]M_B^2, & \beta_b &= -(1 - x_1)(x_1 - r_D^2)M_B^2, \\
\beta_c &= -(1 - x_1 - x_2)[1 - x_1 - x_3(1 - r_D^2)]M_B^2, \\
\beta_d &= (1 - x_1 - x_2)[x_1 - x_3 - r_D^2(1 - x_3)]M_B^2, \\
\beta_e &= [r_c^2 - x_3 - (1 - x_3)r_D^2]M_B^2, & \beta_f &= -x_2(1 - r_D^2)M_B^2, \\
\beta_g &= [r_c^2 - (x_1 - x_3(1 - r_D^2))(x_1 - x_2)]M_B^2, \\
\beta_h &= [r_b^2 - (1 - x_1 - x_3 + x_3 r_D^2)(1 - x_1 - x_2)]M_B^2. \tag{B3}
\end{aligned}$$

The Sudakov factors used in the text are defined by

$$\begin{aligned}
S_{ab}(t) &= s\left(\frac{M_B}{\sqrt{2}}x_1, b_1\right) + s\left(\frac{M_B}{\sqrt{2}}x_2, b_2\right) + \frac{5}{3} \int_{1/b_1}^t \frac{d\mu}{\mu} \gamma_q(\mu) + 2 \int_{1/b_2}^t \frac{d\mu}{\mu} \gamma_q(\mu), \\
S_{cd}(t) &= s\left(\frac{M_B}{\sqrt{2}}x_1, b_2\right) + s\left(\frac{M_B}{\sqrt{2}}x_2, b_2\right) + s\left(\frac{M_B}{\sqrt{2}}x_3, b_3\right) + s\left(\frac{M_B}{\sqrt{2}}(1-x_3), b_3\right) \\
&\quad + \frac{11}{3} \int_{1/b_2}^t \frac{d\mu}{\mu} \gamma_q(\mu) + 2 \int_{1/b_3}^t \frac{d\mu}{\mu} \gamma_q(\mu), \\
S_{ef}(t) &= s\left(\frac{M_B}{\sqrt{2}}x_2, b_2\right) + s\left(\frac{M_B}{\sqrt{2}}x_3, b_3\right) + s\left(\frac{M_B}{\sqrt{2}}(1-x_3), b_3\right) \\
&\quad + 2 \int_{1/b_2}^t \frac{d\mu}{\mu} \gamma_q(\mu) + 2 \int_{1/b_3}^t \frac{d\mu}{\mu} \gamma_q(\mu), \\
S_{gh}(t) &= s\left(\frac{M_B}{\sqrt{2}}x_1, b_1\right) + s\left(\frac{M_B}{\sqrt{2}}x_2, b_2\right) + s\left(\frac{M_B}{\sqrt{2}}x_3, b_2\right) + s\left(\frac{M_B}{\sqrt{2}}(1-x_3), b_2\right), \\
&\quad + \frac{5}{3} \int_{1/b_1}^t \frac{d\mu}{\mu} \gamma_q(\mu) + 4 \int_{1/b_2}^t \frac{d\mu}{\mu} \gamma_q(\mu),
\end{aligned} \tag{B4}$$

where the functions $s(Q, b)$ are defined in Appendix A of [8]. $\gamma_q = -\alpha_s/\pi$ is the anomalous dimension of the quark.

Appendix C: Light-Cone Distribution Amplitudes

Here, we specify the light-cone distribution amplitudes (LCDAs) for pseudoscalar and vector mesons. The expressions of twist-2 LCDAs are [7]

$$\begin{aligned}
\phi_P^A(x) &= \frac{f_P}{\sqrt{6}} 3x(1-x) [1 + a_1^P C_1^{3/2}(t) + a_2^P C_2^{3/2}(t) + a_4^P C_4^{3/2}(t)], \\
\phi_V(x) &= \frac{f_V}{\sqrt{6}} 3x(1-x) [1 + a_{1V}^{\parallel} C_1^{3/2}(t) + a_{2V}^{\parallel} C_2^{3/2}(t)], \\
\phi_V^T(x) &= \frac{f_V^T}{\sqrt{6}} 3x(1-x) [1 + a_{1V}^{\perp} C_1^{3/2}(t) + a_{2V}^{\perp} C_2^{3/2}(t)],
\end{aligned} \tag{C1}$$

and those of twist-3 ones are

$$\begin{aligned}
\phi_P^P(x) &= \frac{f_P}{2\sqrt{6}} [1 + (30\eta_3 - \frac{5}{2}\rho_P^2) C_2^{1/2}(t) - (\eta_3\omega_3 + \frac{9}{20}\rho_P^2(1 + 6a_2^P)) C_4^{1/2}(t)], \\
\phi_P^t(x) &= \frac{f_P}{2\sqrt{6}} [1 + 6(5\eta_3 - \frac{1}{2}\eta_3\omega_3 - \frac{7}{20}\rho_P^2 - \frac{3}{5}\rho_P^2 a_2^P)(1 - 10x + 10x^2)], \\
\phi_V^t(x) &= \frac{3f_V^T}{2\sqrt{6}} t^2, \phi_V^s(x) = -\frac{3f_V^T}{2\sqrt{6}} t, \phi_V^v(x) = \frac{3f_V^T}{8\sqrt{6}} (1 + t^2), \phi_V^a(x) = -\frac{3f_V^T}{4\sqrt{6}} t,
\end{aligned} \tag{C2}$$

where $t = 2x - 1$, f_V and f_V^T are the decay constants of the vector meson with longitudinal and transverse polarization, respectively. For all pseudoscalar mesons, we choose $\eta_3 =$

0.015 and $\omega_3 = -3$ [26]. The mass ratio $\rho_{\pi(K)} = m_{\pi(K)}/m_0^{\pi(K)}$ and $\rho_{\eta_q(s)} = 2m_{q(s)}/m_{qq(ss)}$, and the Gegenbauer polynomials $C_n^\nu(t)$ read

$$\begin{aligned} C_2^{1/2}(t) &= \frac{1}{2}(3t^2 - 1), & C_4^{1/2}(t) &= \frac{1}{8}(3 - 30t^2 + 35t^4), & C_1^{3/2}(t) &= 3t, \\ C_2^{3/2}(t) &= \frac{3}{2}(5t^2 - 1), & C_4^{3/2}(t) &= \frac{15}{8}(1 - 14t^2 + 21t^4). \end{aligned} \quad (C3)$$

-
- [1] N. Brambilla et al., (Quarkonium Working Group), CERN-2005-005, hep-ph/0412158.
 - [2] Dong-Sheng Du and Z. Wang, Phys. Rev. D **39**, 1342 (1989).
 - [3] Ho-Meoyng Choi and Chueng-Ryong Ji, Phys. Rev D **80**, 114003.
 - [4] Ho-Meoyng Choi and Chueng-Ryong Ji, Phys. Rev D **80**, 054016 (2009).
 - [5] Jia-Fu Liu and Kuang-Ta Chao Phys. Rev. D **56**, 4133 (1997); M. A. Ivanov, J. G. Korner and P. Santorelli, Phys. Rev. D **73**, 054024 (2006).
 - [6] Junfeng Sun, Yueling Yang, Wenjie Du, and Huilan Ma, Phys. Rev. D **77**, 114004 (2008).
 - [7] Xin Liu, Zhen-Jun Xiao, and Cai-Dian Lü, Phys. Rev. D **81**, 014022 (2010).
 - [8] Jian-Feng Cheng, Dong-Sheng Du, and Cai-Dian Lü Eur. Phys. J. C. **45**, 711 (2006).
 - [9] Junfeng Sun, Dong-sheng Du, Yueling Yang, Eur. Phys. J. C. **60**, 107 (2009).
 - [10] Jun Zhang, Xian-Qiao Yu, Eur. Phys. J. C. **63**, 435 (2009).
 - [11] Hai-Yang Cheng and Chun-Khiang Chua, Phys. Rev. D **80**, 114008 (2009).
 - [12] Dong-Sheng Du and Zheng-Tao Wei, Eur. Phys. J. C. **5**, 705 (1998).
 - [13] Zhen-Jun Xiao and Xin Liu, Phys.Rev. D **84**, 074033 (2011).
 - [14] Y. Y. Keum, H. n. Li and A. I. Sanda, Phys. Lett. B **504**, 6 (2001) [arXiv:hep-ph/0004004]; C.-D. Lü, K. Ukai, M.Z. Yang, hep-ph/0004213, Phys. Rev. D **63**, 074009 (2001); C.-D. Lü, M.Z. Yang, Eur. Phys. J. C. **23**, 275 (2002).
 - [15] B.H. Hong and C.D. Lu, Sci. China G **49**, 357-366 (2006).
 - [16] Run-Hui Li, Cai-Dian Lü, and Hao Zou, Phys. Rev. D **78**, 014018 (2008); Run-Hui Li, Cai-Dian Lü, A.I. Sanda and Xiao-Xia Wang, Phys. Rev. D **81**, 034006 (2010).
 - [17] Hao Zou, Run-Hui Li, Xiao-Xia Wang, and Cai-Dian Lü, J. Phys. G: Nucl. Part. Phys. **37**, 015002 (2010).
 - [18] Ying Li, Cai-Dian Lü and Cong-Feng Qiao, Phys.Rev.D **73**,094006 (2006); Ying Li and Cai-Dian Lü, J.Phys.G **29**, 2115 (2003); Ying Li, Cai-Dian Lü and Zhen-Jun Xiao, J.Phys.

- G **31**, 273 (2005).
- [19] Yong-Yeon Keum, T. Kurimoto, Hsiang-nan Li, Cai-Dian Lü and A.I. Sanda, Phys. Rev. D **69**, 094018 (2004).
 - [20] Cai-Dian Lü, Eur. Phys. J. C **24**, 121 (2002).
 - [21] T. Kurimoto, H. n. Li and A. I. Sanda, Phys. Rev. D **67**, 054028 (2003).
 - [22] G. Buchalla, A.J. Buras, M.E. Lautenbacher, Rev. Mod. Phys. **68**, 1125 (1996).
 - [23] M. Beneke, G. Buchalla, M. Neubert, and C.T. Sachrajda, Phys. Rev. Lett. **83**, 1914 (1999); Nucl. Phys. B **591**, 313 (2000).
 - [24] C.W.Bauer, S. Fleming, D. Pirjol and I. W. Stewart, Phys. Rev. D **63**, 114020 (2001) [arXiv: hep-ph/0011336]; C.W.Bauer, D. Pirjol and I. W. Stewart, Phys. Rev. Lett. **87**, 201806 (2001) [arXiv: hep-ph/0107002].
 - [25] J. C. Collins and D. E. Soper, Nucl. Phys. B **193**, 381 (1981); J. Botts and G. Sterman, Nucl. Phys. B **325**, 62 (1989).
 - [26] V.M. Braun and I.E. Filyanov , Z. Phys. C **48**, 239 (1990); P. Ball, V.M. Braun, Y. Koike, and K. Tanaka, Nucl. Phys. B **529**, 323 (1998); P. Ball, J. High Energy Phys. **01**, 010 (1999).
 - [27] Cai-Dian Lü, M.-Z. Yang, Eur. Phys. J. C **28**, 515 (2003).
 - [28] A. V. Manohar and M. B. Wise, Camb. Monogr. Part. Phys. Nucl. Phys. Cosmol. **10**, 1 (2000).
 - [29] B. Melic, B. Nizic, and K. Passek, Phys. Rev. D **60**, 074004 (1999).
 - [30] Th. Feldmann, P. Kroll, and B. Stech, Phys. Rev. D **58**, 114006 (1998).
 - [31] R. Escribano and J.M. Frere, J. High Energy Phys. **06** (2005) 029; J. Schechter, A. Subbaraman, and H. Weigel, Phys. Rev. D **48**, 339 (1993).
 - [32] Particle Data Group, J. Phys. G: Nucl. Part. Phys. **37**, 075021 (2010).
 - [33] P.Ball and R. Zwicky, Phys. Rev. D **71**, 014015 (2005); P. Ball and R. Zwicky, J. High Energy Phys. **04** (2006); P. Ball and G.W. Jones, J. High Energy Phys. **03**, 069 (2007).
 - [34] W. Wang, Y.-L. Shen, C.-D. Lu, Phys. Rev. D **79** (2009) 054012, e-Print: arXiv: 0811.3748 [hep-ph]
 - [35] A. Ali, G. Kramer and C.-D. Lü, Phys. Rev. D **58**, 094009 (1998); Yaw-Hwang Chen, Hai-Yang Cheng, B. Tseng, and Kwei-Chou Yang, Phys. Rev. D **60**, 094014 (1999).
 - [36] Sebastien Descotes-Genon, Jibo He, Emi Kou and Patrick Robbe, Phys. Rev. D **80** 114031

(2009).

- [37] Ying Li and Cai-Dian Lü, Phys. Rev. D **73**, 014024 (2006).
- [38] C.-H. Chen, Y.-Y. Keum and H.-N. Li, Phys. Rev. D **66**, 054013 (2002).
- [39] Han-Wen Huang, Cai-Dian Lü, Toshiyuki Morii, Yue-Long Shen, Ge-Liang Song and Jin Zhu, Phys. Rev. D **73**, 014011 (2006).